Fabrication and Characterization of 3D Printed Scaffold based on PLA/TCP for Bone Tissue Engineering

Jung Hong-Hee

Department of Graduate Program of Biomedical Engineering
The graduate School, Yonsei University

Fabrication and Characterization of 3D Printed Scaffold based on PLA/TCP for Bone Tissue Engineering

Directed by Professor Jong-Chul Park

Doctoral Dissertation
Submitted to the Department of Graduate Program of
Biomedical Engineering,
the Graduate School of Yonsei University
in partial fulfillment of the requirements for the degree of

Doctor of Philosophy of Biomedical Engineering

Jung Hong-Hee

August 2016

This certifies that the Doctoral Dissertation of Jung Hong-Hee is approved.

_____

Thesis Supervisor : Jong-Chul Park

_____

Thesis Committee Member #1: Yoo Sun Kook

_____

Thesis Committee Member #2: Kim Nam Hyun

_____

Thesis Committee Member #3: Park, Kwideok

_____

Thesis Committee Member #4 : Yang, Hee Seok

The Graduate School
Yonsei University
August 2016

TABLE OF CONTENTS

LIST OF FIGURES

LIST OF TABLES

ABSTRACT

Fabrication and Characterization of 3D Printed Scaffold based on PLA/TCP for Bone Tissue Engineering

Jung Hong-Hee

Dept. of Graduate Program of Biomedical Engineering

The Graduate School

Yonsei University

Medical advances have led to a welcome increase in life expectancy. However, accompanying longevity introduces new challenges: increases in age-related diseases and associated reductions in quality of life. The loss of skeletal tissue that can accompany trauma, injury, disease or advancing years can result in significant morbidity and significant socio-economic cost and emphasise the need for new, more reliable skeletal regeneration strategies. To address the unmet need for bone augmentation, tissue engineering and regenerative medicine have come to the fore in recent years with new approaches for de novo skeletal tissue formation. Typically, these approaches seek to harness stem cells, innovative scaffolds and biological factors that promise enhanced and more reliable bone formation strategies to improve the quality of life for many. Synthetic bone substitutes provide an alternative to the limited resources of autografts and the problems which arise when using allogenic and xenogenic grafts. The successful implantation of a biomaterial into bone is determined by the intimate interaction between the implant and the host tissue at the implant/tissue interface. The

process of bone cell ingrowth is highly influenced by surface properties and the architecture of the scaffold. A bone graft material should therefore possess sufficient porosity and permeability to allow integration within the native tissue and vascular invasion, and it must satisfy the transport demands for oxygen and nutrients. Porous bone scaffolds can be made by a variety of methods. Chemical/gas foaming, solvent casting, particle/salt leaching, freeze drying, thermally induced phase separation, and foam-gel are some of those that have been used extensively. However, the production of a scaffold with complicated and irregular geometry can be limited by conventional scaffold fabrication techniques. Also, pore size, shape, and its interconnectivity cannot be fully controlled in these approaches. Therefore, recent research efforts have focused on the fabrication of a scaffold with complicated and interconnected pore structure, including several computer-designed scaffold fabrication techniques. In this study, to provide bone grafts of synthetic calcium phosphates (CaP) and PLA(Poly lactic acid), three-dimensional (3D) printing have been used to realize 3D bone-like structures. These technologies allow the design and fabrication of complex scaffold geometries with a fully interconnected pore network. The objective of this research was to carry out an in vitro and in vivo study of the biological performance of 3D printed PLA/β-TCP composite material, to estimate the scope of their potential applications in bone surgery. Samples with increasing β-TCP(0-70% w/w) contents were processed by 3D plotting system. The chemical composition and surface properties of 3D printed PLA/β-TCP were characterized by FT-IR, TGA and SEM. In vitro studies were also done to evaluate the biomineralization activity and the cytotoxic profile of the scaffolds. The in vivo study was carried out using of composite materials composed composite materials containing 50 or 70% β-TCP and pure β-TCP, respectively. This study showed that adding increasing percentages of β-TCP to a lactic acid polymer matrix stimulated the proliferation

of mouse osteoblast cells and synthesis of the extracellular bone matrix in a dose-dependent manner. In vivo results indicate that, the composite materials containing 70% β-TCP demonstrated a higher performance in terms of osteogenesis.

Key words : Poly(lactic acid), β-tricalcium phosphate, three-dimensional printing, tissue engineering, osteogenic

I. INTRODUCTION

1. Anatomy and function of bone

Bone is a biological composite comprising 90% extracellular matrix(ECM) and 10% water.[1] The ECM is composed of 60～70% inorganic mineral usually referred to as hydroxyapatite(HA) which has a similar, but not identical structure to natural bone mineral. HA has a chemical formula of $Ca_{10}(PO_4)_6(OH)_2$ and a Calcium Phosphorus(Ca:P) ratio of 5:3(1.66). Bone apatite is characterised by calcium, phosphate, and hydroxyl deficiency with typical Ca:P ratios between 1.37 and 1.87.[2] The remaining 30～40% of bone ECM contains organic components composed of type I collagen(90%) with non-collagenous proteins glycosaminoglycans(GAGs). The collagen confers flexibility and fracture toughness to the matrix and the inorganic phase confers stiffness. Macroscopically two types of bone exist. Cortical bone forms the outer shell of all bones and has a dense structure representing approximately 80% of skeletal mass. Cancellous bone has a porous structure and is found in the centre of all bones. It demonstrates the layout of cortical and trabecular bone within the tibia as well as the important anatomical features. Figure 1 showed a detailed section through the bone demonstrates the porous sponge-like structure of trabecular bone surrounded by dense cortical bone.

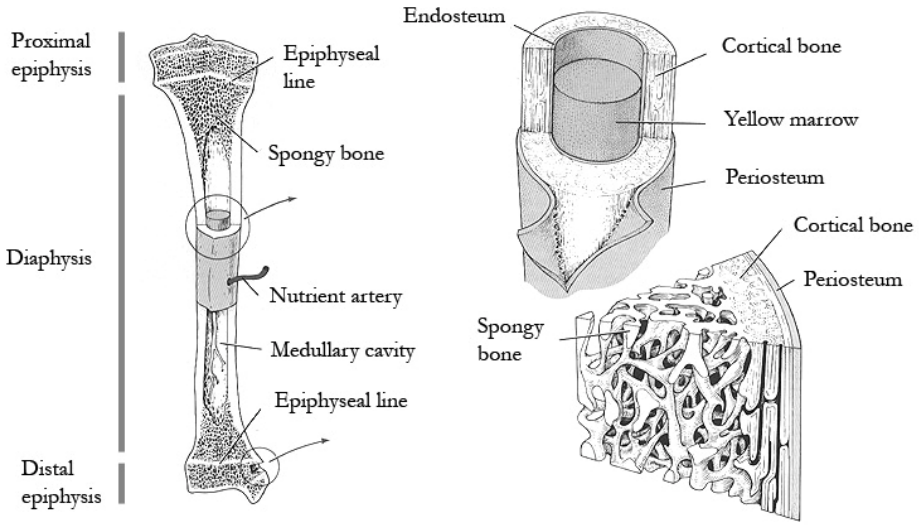

Fig. 1. An anatomical drawing of a human tibia[3]

Adult bone contains four cell types each with a specific set of functions. Osteoprogenitor cells are mesenchymal cells of bone. They differentiate into osteoblasts when new bone is required, or lie quiescent and are known as bone lining cells when bone is not needed. Osteoblasts are bone forming cells that deposit osteoid matrix onto the collagen fibres and control the subsequent mineralisation of woven bone into lamellar bone. Osteocytes are osteoblasts that have become entombed by mineralized matrix and may remain in this state for

years and even decades. Osteocytes regulate the composition of bone matrix via ionnutrient exchange thus maintaining the calcium and phosphate levels in serum. Osteoclasts are large, multinucleated cells able to break down calcified bone matrix. They originate from haemopoietic progenitor cells and can attach themselves to bone where they erode it via acidic digestion.[4] Bone is laid down in a highly ordered manner in vivo, where osteoblasts lay down bone in the space created by previous osteoclast resorption. Thus, the structure and morphological layout of the bone is preserved.[5] Bone can only be formed by deposition on a suitable surface that is within 200 μm of a blood supply so that it can receive nutrients via diffusion. These two criteria place limitations on the shape and size of developing bone which may form either by intramembranous ossification or endochondral ossification. Intramembranous ossification starts after 6.5 weeks of gestation and occurs when a primary ossification centre develops in a slab of mesenchyme tissue. Here bone forming cells differentiate from mesenchymal cells and bone is formed without the need for cartilage. Endochondral ossification occurs by calcification of cartilage tissue. This occurs during growth of the foetal skeleton where the limbs need to grow in length and diameter. Bones are rigid and not able to achieve this; therefore cartilage is formed as an intermediary tissue and later calcified. Regions of cartilage persist on the bone ends and within the epiphyseal growth plate until bone stops growing in late adolescence.[4,6] Bone remodelling is a continual process of resorption and renewal that continues throughout the life of all mammals. It is defined as removal and replacement of bone tissue without altering its overall shape. The mechanical properties of bone are remarkable and make it challenging to replicate. It possesses excellent strength, stiffness, and fracture toughness whilst also being porous and able to support the growth of cells and repair itself. Its properties derive from the size, shape, and organisation of the mineral and matrix phases throughout its structural

hierarchy.[7] There is a large variation in the reported properties of bone due to many factors including its anisotropy, person to person variation, use of aged or osteoporotic bone, and the anatomical location of the tested specimen.[8,9] The compressive modulus for cortical bone lies in the range 5~35 GPa and compressive strength 50~250 MPa. The tensile modulus varies from 4~30 GPa and tensile strength 90~170 MPa.[9-14] It is important for any implant replacing bone to match both the strength and stiffness of the native bone to prevent problems with stress shielding and excessive movement. Both may lead to resorbtion of the native bone and failure of the implant.[9] Table 1 provides a summary of the strength and modulus values for cortical and cancellous portions of human long bones.[13] It is immediately apparent that cortical bone is at least an order of magnitude stronger and stiffer than cancellous bone. This is due to the differing levels of porosity with cancellous bone having significantly greater porosity(30-90%) compared with cortical bone(8-28%). The minimum mechanical properties for a structural bone graft material are a compressive modulus of approximately 5 GPa, tensile strength ~90 MPa and compressive strength ~90 MPa.

Table 1. Summary of human long bone mechanical properties[9-14]

	Cortical bone	Cancellous bone
Compressive Strength (MPa)	50 - 250	1.5 - 10
Compressive Modulus (GPa)	5 - 35	0.05 - 0.9
Tensile strength (MPa)	90.6 - 170	-
Tensile modulus (GPa)	3.9 - 29.2	-
Torsion strength (MPa)	3.1 - 7.4	-
Torsion modulus (GPa)	5 - 71	-
Bending strength (MPa)	103 - 238	-
Bending modulus (GPa)	68 - 98	-
Bulk porosity (%)	8 - 28	30 - 90
Pore size range (μm)	5 - 200	1 - 900

Healing is the natural response to injury through which dead tissue is replaced by living tissue and bone possesses the ability to heal itself. Fracture healing occurs in two ways: with callus and without. Healing with callus typically occurs in tubular bones in the absence of rigid fixation. The precise number of defined stages in the healing process varies depending on author[16-18] but typically the process of fracture healing occurs in five stages. First is tissue destruction and haematoma formation where the damaged blood vessels form a haematoma within and around the fracture site, whilst bone at the fracture surfaces dies as a result of the loss of blood supply. The next stage is inflammation and cellular proliferation which occurs within 8 hours of the fracture. During this stage there is inflammation and proliferation of cells surrounding the fracture. The clotted haematoma is slowly absorbed and infiltrated by blood vessels and a callus forms around the fracture. Osteoclasts now begin to remove dead bone whilst osteogenic

and chondrogenic cells create immature or 'woven' bone from the callus. Over time the callus is progressively mineralised eventually uniting the fracture. The woven bone is then consolidated into lamellar bone by the action of osteoblasts and osteoclasts. This process is slow and it may be months before the bone is strong enough to carry normal loads. Finally remodelling occurs over a period of years to remove excess bone laid down during the healing process and strengthen the union. Healing without callus occurs when the fracture site is immobile as in the case of internal fixation. It occurs in the same manner except that a large callus does not form since it is not required to maintain the integrity of the fracture. The rate of fracture healing will depend on the type of bone involved (cancellous bone heals faster than cortical bone), the state of the blood supply (poor circulation results in slow healing), the patient's general health, and finally the age of the patient. Healing can be twice as fast in children as in adults. For the majority of simple fractures bone healing will proceed normally within a period of weeks or months. However problems with non union occur in up to 10 % of cases and there are many other instances in which larger bone defects occur that require surgical intervention.[19] All bodily organs including bone are susceptible to pathological conditions and age related degeneration that may require repair through surgical reconstruction. Defects in bone arise principally as a result of disease, trauma, infection or genetic abnormality.[20] When these defects go beyond a 'critical' size they will not heal spontaneously and any void will be rapidly filled with fibrous tissue produced by fibroblasts. These are present throughout the body and are able to proliferate rapidly. Once this fibrous connective tissue is present it prevents any tissue repair or replacement from taking place. Thus, biodegradable membranes, scaffolds, and graft materials are essential to prevent undesirable tissue ingrowth and enable the body to heal critical sized bone defects. There are an enormous number of diseases and bone disorders which may lead to the

requirement for bone graft including neurological afflictions(poliomyelitis, cerebral palsy and spina bifida), endocrine disorders (osteoporosis, hypopituitarism and acromegaly), metabolic bone diseases (osteomalacia, rickets and hyperparathyroidism), abnormal bone development(achondroplasia or osteogenesis aclasis), bone disorders (cystic changes or tumours) or spinal conditions (degenerative disc disease, spondylolisthesis or scoliosis). Cancer often leads to the need for limb amputations although recent advances in the staging, diagnostic imaging and treatment of musculoskeletal sarcomas has led to an increase in the number of limb salvage operations (up to 90 %) as an alternative to amputation. The survival rate for limb sparing surgery has been shown to be similar to those treated with amputation. Local resection of the tumour and reconstruction has become the most common route for management of bone tumours.[21-23] In the case of traumatic injuries where the patient is in otherwise good health then healing of major injuries should proceed normally. Complications may occur when these injuries are combined with other diseases, infection or disruption to the blood supply (avascular necrosis, osteonecrosis, aseptic necrosis or ischemic bone necrosis). This usually occurs at the ends of long bones as a result of traumatic disruption to the blood supply, from long term use of medications (cortico steroids) or excessive long term alcohol consumption. Infection of bone (osteomyelitis) is classified into acute and chronic. Acute osteomyelitis occurs when bacteria, typically staphylococcus aureus enter the bone via the blood stream. It causes severe pain and tenderness over the involved bone accompanied by a fever. The bacteria multiply in the bone causing pus to form which eats away at the bone and causes an abscess. Treatment via antibiotics, surgical drainage and curettage is usually successful although chronic osteomyelitis may develop from unsuccessful treatment of acute symptoms, surgery or open fractures where the bone has become contaminated.[24] In severe cases the bone requires

resection and replacement with graft material or other implant. If the infection persists amputation may be required. In the same way that there a great number of diseases which affect humans there are also a large number of bone abnormalities that may arise from genetic or environmental circumstances. These may lead to under or over production of bone(fibrodysplasia ossificans progressiva), weak bones(osteogenesis imperfecta) or unusual growth of bones. Any one of these situations may require surgical intervention with the use of bone graft to correct.

2. Current bone grafting solutions

Historically, orthopaedic reconstruction has made extensive use of non degradable materials e.g. stainless steel, titanium, or alumina to replace bone tissue. These devices are associated with long term problems such as loosening, fracture, and the biological reaction to wear debris and metallic ion release.[21] In order to spare the patient from a retrieval operation and reduce the overall resource required to carry out this procedure, considerable effort is being directed towards the development of degradable implants. This modern approach is marked by a shift in emphasis from replacement to regeneration of tissues by use of materials which degrade over a period of time and are replaced by native tissue.[25] When a bone graft is required the primary route for the surgeon is to transplant bone from another site on the same individual for use at the defect site, this is known as autograft. When this is not available bone donated from another member of the same species (allograft), from another species (xenograft) usually porcine or bovine in origin, or synthetic materials may be used.[26] Since 1940 autografting has been used extensively in maxillofacial surgery but it was not until the 1980s that allograft bone banking, vascularised autograft and bone graft substitutes became

routinely available.[26,27] Autograft is considered as the 'gold standard' in terms of performance. This technique promotes osteogenesis, osteoinduction and osteoconduction. Osteogenesis is the creation of new bone via cells and proteins within the graft, osteoinduction is the biologically mediated recruitment or differentiation of pluripotent cells into chondrocytes and osteoblasts essential for bone formation and osteoconduction is the facilitation of blood vessel ingrowth into a three dimensional (3D) scaffold.[23,28,29] Autograft has no associated risk of viral transmission, excellent success rates, offers structural support and is eventually remodelled into the surrounding bone through creeping substitution. Unfortunately, there are few sites from which bone can be harvested without serious complications. The iliac crest is most commonly used but bone can also be harvested from Gerdy's tubercle, the distal radius, and the distal tibia. Its availability is limited, and often severely limited when it is required for the most challenging cases. Autograft harvest requires a separate surgical procedure with associated risks, costs and time.[2] Furthermore autograft is associated with 8.5–20 % risk of complications which include blood loss, nerve 26 injury, hernia formation, infection, arterial injury, fracture, cosmetic defects and chronic pain.[33,34] Allograft is available off the shelf from bone banks in a number of geometric forms and has excellent mechanical properties although these vary from batch to batch. It has been associated with delayed healing, poor remodelling[32], and disease transmission.[33] There have been reported cases of HIV transmission and bacterial contamination from allograft bone. As a result, bone banks now undertake secondary sterilisation although this degrades the mechanical properties of the bone. Both allograft and xenograft are highly immunogenic and can stimulate a potent incompatibility reaction. This can be improved by processing the bone, for example by freezing, freeze drying, gamma irradiation or chemical means. This eliminates any osteogenic capacity leaving only an osteoconductive scaffold.

Xenograft has similar performance to allograft but with the additional risk of animal derived diseases including bovine spongiform encephalopathy(BSE).[26] The drawbacks with conventional grafting methods have led to a great deal of research and development into synthetic alternatives known as bone graft substitutes or bone scaffolds. These can be broadly classified by their constituent material: polymer(synthetic and natural), ceramic, glass or a composite of two or more. The most common polymeric materials in use belong to the polyester family and a subset of this the poly(α-hydroxyacids). These contain polylactide (PLA) and polyglycolide (PGA) which have excellent mechanical properties and can be combined to alter the rate of degradation. They degrade to monomeric acids and then carbon dioxide via respiration and the citric acid cycle in the kidneys.[34,35] These degradation products are acidic and may lead to a local decrease in pH around an implant and subsequent cell lysis. For this reason they are often combined with calcium phosphate filler materials hydroxyapatite(HA) or tricalcium phosphate (TCP) which serve to reinforce the matrix and neutralise the surrounding environment due to their basic degradation products.[36-38] The calcium phosphates have also been used on their own because of their excellent biocompatibility and osteoconductivity. Recent work has determined that macrostructure, microstructure, and chemical composition are critical to their osteoinductive potential although the precise mechanisms behind this are not fully understood.[30,39,40] Of the glassy materials, the most famous is Bioglass® developed by Hench et al in 1969 and available in resorbable and non resorbable variants.[41] It exhibits a strong bond to bone, has been shown to upregulate the expression of genes related to osteoblast activity[42,43], and has found extensive use in maxillofacial and dental applications. Its moderate mechanical properties limit its use as a bone graft substitute for load bearing applications. The principal advantages of bone graft substitute are unlimited supply, easy sterilization and

storage, predictable mechanical properties, excellent bone ingrowth and moderate cost.[44] There is an ever expanding choice of bone graft substitute available on the market, typically in the form of powders, granules or blocks. These are summarised in Table 2 which elucidates the manufacturer and brand name, material, published information on porosity and strength and approved indications. Establishing the cost for each bone graft substitute proved extremely challenging since the price paid varies between institutions and as such they are commercially sensitive. The majority of these bone graft substitute materials are indicated as fillers for bony defects which are not intrinsic to the stability of the skeleton, those that are able to offer some structural support for the skeleton are dense materials. Few are indicated for use at infected sites or in the presence of systemic disease. Load bearing capacity is not essential for all indications particularly if the material is mixed with bone marrow aspirate and allowed to clot before use. This forms a highly osteoinductive bone graft with excellent handling properties, able to fill large non structural defects after revision hip arthoplasty and posterolateral lumbar fusions.

Table 2. Bone graft substitute materials available in the market in 2009

Manufacturer & brand name	Availablility	Material	Strength	Porosity	Structural
AAP					
Cerabone	granules and blocks	Bovine derived HA	Low	100 - 1500 μm	N
Ostim	Injectable paste	HA	Moderate	N/A	N
PerOssal	Porous morsels	Nano HA	N/A	High	N
Apatech					
Actifuse	Granules, mouldable paste	Si substituted HA	N/A	High	N
Berkeley advanced biomaterials					
Bi-Ostetic	Blocks and granules	60% HA 40% β-TCP	N/A	high	N
Cem-Ostetic	Injectable paste	Nano HA	Low	N/A	N
GenerOs	Granules	B-TCP	N/A	high	N
Biocomposites					
Stimulan	Pellets or injectable paste	Calcium Sulphate	N/A	N/A	N

Allogran N	pellets	HA	N/A	N/A	N
Allogran R	pellets	β-TCP	N/A	N/A	N
Gene X	Injectable paste	Biphasic CaP	N/A	N/A	N

There is currently a need for structural synthetic bone graft materials that can be used as a substitute to allogenous or autogenous graft materials in large defects, for example in resections for infection or tumour. In these instances bone grafts can be as large as 20cm and their location(joints, spine, and long bones) require them to be able to bear load and be used with instrumentation to maintain the stability of the skeleton. A graft material capable of replicating the properties of allograft without its inherent risks would represent a major step forward in bone grafting. Furthermore, a bone graft substitute material with cortical bone matching mechanical properties may prove beneficial in other indications interbody spinal fusion where high strength and osteoinductivity are required to ensure rapid fusion. An important area for consideration is how the healing environment alters according to anatomical location metaphyseal defects, long-bone fractures, interbody spine fusion or posterolateral spine fusion. Each will have different levels of difficulty in forming new bone, metaphyseal defects may only require an osteoconductive material whereas a posterolateral fusion will not succeed with a purely osteoconductive material as a result of the poorer blood supply. A poorly vascularised site will lead to problems with nutrient diffusion into the graft and affect the maximum size of the defect that can be successfully treated.[28] Therefore, it is important to validate that a material will work as intended for each site into which it is implanted.[23] In challenging cases it is often not enough

to use a purely osteoconductive material and new techniques are required, for example, tissue engineering. This requires a new and multidisciplinary understanding of materials that considers many new factors which include: developmental biology, genetic engineering, and cell biology as well as the surgical techniques required for their use. A satisfactory outcome when repairing any defect is dependent on restoration of an adequate blood supply and the ability to maintain implant stability and controlled loading whilst repair is underway. Large structural defects present the greatest clinical challenge and in order to improve the chances of successfully repairing them it is necessary to consider the use of tissue engineering.[45]

3. Tissue Engineering

Tissue engineering(TE) is the regeneration of tissues through an in depth understanding of the complex mechanisms and processes occurring in the human body by combining knowledge from many disciplines.[46] Engineers, materials scientists and chemists examine methods to create a bone-like scaffold whilst life scientists examine the body's response to them at the same time as searching for methods to accelerate and improve the likelihood of successful healing. Numerous types of synthetic scaffolds have been fabricated and investigated in the search for effective bone graft substitutes. There are many scaffold design variables that can strongly influence the biologic response including the single or multi-phase composition of the scaffold, surface chemistry, architectural parameters such as pore size and interconnectivity, the rate of degradation and the degradation products, and the local mechanical properties of the matrix such as modulus and viscoelasticity. Structural biomaterial scaffolds that provide adequate mechanical properties must often be surface modified or combined with bioactive components to achieve the desired mix of properties. Dramatic advances in biomaterials

synthesis, biological performance evaluation, and engineering analysis have combined to create unprecedented choices for the selection of scaffold materials.

4. Synthetic bone graft substitute

A synthetic graft material requires suitable mechanical properties to resist the dynamic stresses and strains imposed upon it according to its anatomical location and skeletal movement. It must have a porous surface and completely open porosity with fully interconnected pores to facilitate the ingrowth of bone, initially via angiogenesis and then through the normal bone remodelling process. The rate of degradation needs to occur in a predictable manner in sequence with bony ingrowth and ideally be adjustable to account for patient age, health, smoker or non smoker, anatomical location, and proximity to a good blood supply.[47] A material that maintains strength for a period of time and then completely disintegrates is less preferable to one which steadily declines in strength. An ideal timescale for degradation is regarded to be between 6 and 24 months depending on the likely healing rate. The ability to sterilise the implant without compromising its properties is vitally important to eliminate the risk of infection. The materials that comprise the bone graft substitue should be biocompatible, biodegradable, osteoinductive, osteoconductive and not elicit any unsatisfactory immune responses. β-Tricalcium phosphate(β-TCP) is an osteoconductive, absorbable material, which, in porous ceramic form, is highly suitable for implants used in bone reconstruction or as bone substitutes. β-TCP, used for many years to replace or complement autologous bone in bone grafts, has proved its clinical effectiveness in many indications.[48-52] Like any ceramic material, however, these implants have a brittle fracture behavior. They break suddenly, without any prior plastic strain, which restricts the clinical applications for these materials to surgery with low stress levels. On the other hand, biodegradable polymers from

aliphatic polyesters of α-hydroxy acid derivatives, such as polylactic acid(PLA), evidence a modulus of elasticity closer to that of natural cortical bone and can retain high strength over time.[53] But these materials can induce unspecific inflammatory tissue response,[54-60] resulting in delayed bone healing/fusion or osteolytic reactions.[61-66] To overcome the disadvantages of these different materials, composite materials of calcium phosphates and polyesters have been developed and evaluated in vitro or in vivo.[67-75] Such composite materials tend to increase phenotypic expression of osteogenic cells, reduce foreign-body reaction, and improve bone healing in a dose-dependent manner as compared to pure polymer materials.

5. Three-dimensional printing methods

Porous bone scaffolds can be made by a variety of methods. Chemical/gas foaming[76], solvent casting, particle/salt leaching[77,78], freeze drying[79], thermally induced phase separation[80], and foam-gel[81] are some of those that have been used extensively. However, the production of a scaffold with complicated and irregular geometry can be limited by conventional scaffold fabrication techniques.[82] Also, pore size, shape, and its interconnectivity cannot be fully controlled in these approaches. Therefore, recent research efforts have focused on the fabrication of a scaffold with complicated and interconnected pore structure, including several computer-designed scaffold fabrication techniques. Three-dimensional printing(3DP) was developed at Massachusetts Institute of Technology to build structures from powdered materials.[83-85] First, a thin layer of loose powder particles is spread. Then, selective deposition of liquid binder from an inkjet printhead creates a 2D pattern of bound particles. This process is repeated layer by layer until a 3D object is built. Parts are removed from the powder bed and unbound powder is

removed. These pioneering techniques can be used to fabricate a customized and solvent-free scaffold with tailed bone geometry and interconnected pore structures for repair of bone defects.

6. Objective

The first aim of this work the fabrication of a computer-designed and solvent-free PLA/TCP scaffold using 3DP to provide several potential advantages such as ease of customized manufacture and in vivo osteogenesis because there was no study regarding to utilization of PLA/TCP composite scaffold with different contents of β-TCP for bone defect using 3DP.

PLA is known that before the polylactone-type polymer metabolized into carbon dioxide and water, the degradation products of the polymers are lactic acid and glycolic acid, both acidic. Accumulation of the acidic matter could induce bacteria-free inflammation of the surrounding tissue. In this study, β-TCP was selected as an alkaline component to overcome the acidity of degradation products of the polymer. Thus, the second aim of this work was determined in vitro degradation rate and acidity of the degradation system of the composite scaffold and compared with that of β-TCP free PLA scaffold.

The basic approach of bone tissue engineering includes creating neo-bone tissue within implanted biodegradable polymeric scaffolds in vivo. Few studies have examined the in vivo correlation between scaffold degradation and formation of neo-bone tissue.[86] Based on this concept, the third aim of this work was to understand whether 3DP fabricated PLA/TCP scaffold(3DP PLA/TCP) degraded over the appropriate experimental time frame to guide the formation of neo-bone tissue into the cranial bone defects.

II. MATERIALS & METHODS

1. Fabrication of 3DP PLA/TCP composite Scaffold

1.1. Materials

A commercial bioresorbale polymer, Poly(L-lactic-acid)(PLA, Evonik industries, germany) was used without further purification. It was characterized by an intrinsic viscosity of 1.4 dL/g and a melting temperature of 181.7℃. PLA is known to be a very hydrophilic polymer, and was dried overnight at 105℃ under vacuum before processing. β-TCP powders were purchased from the Sigma - Aldrich Co. (USA) The grain size of the TCP powder was ~100 nm(reported by the manufacturer).

1.2. Printing of 3DP PLA/TCP composite scaffolds

The 3D plotting (ProtekKorea; Daejeon, Korea) consisted of a plotting system with a heating jacket and a stainless steel cylinder with a micronozzle moved by an air dispenser in the direction of the x - y - z stage. The plotting system was controlled by Scaffold Path Generation SW computer software (Korea Institute of Machinery and Materials; Daejeon, Korea). The computer-designed circular 3DP scaffold was fabricated using a blend of PLA and β-TCP by Multi-Head Deposition System.(Fig. 2.)

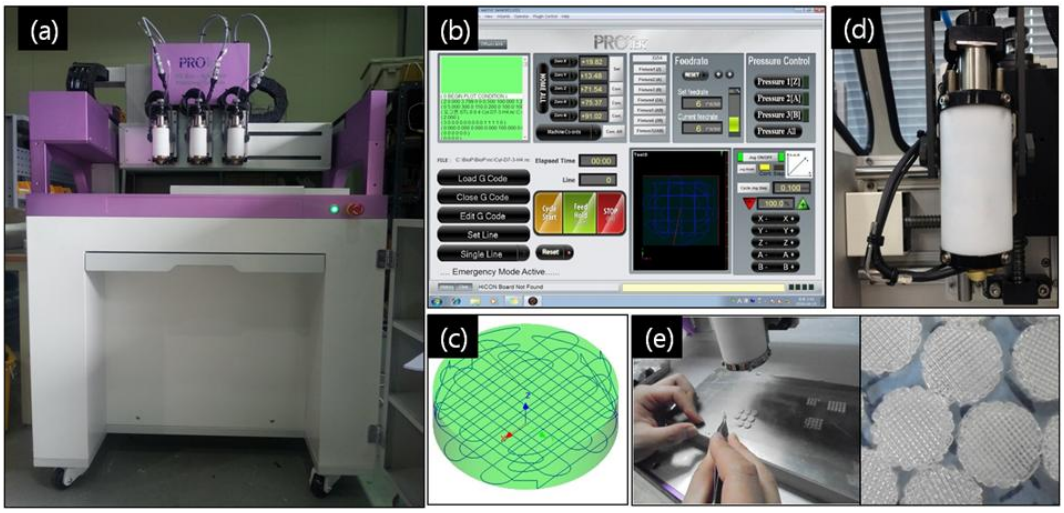

Fig. 2. (a) SFF 3D Plotter system , (b,c) Scaffold Path Generation SW computer software, (d,e) Fabrication process of the PLA/TCP scaffold using a 3D plotting system

The PLA/TCP mixture was prepared by adding 30, 50 and 70%(wt%) powdered β-TCP to the PLA polymer using a freezer mill.(Fig. 3.)

Fig. 3. Mixing process of the PLA and β-TCP powder using a freezer mill

The prepared mixture was placed in a 50 mL steel syringe fastened to the 3D plotter, and dispensed through a steel nozzle at temperature >180 ℃ by applying a pneumatic pressure of 600 kPa; the feed rate was 100 mm/min. Disc shaped PLA/TCP scaffolds(diameter, 8.0 mm; height, 2.0 mm) were fabricated having line width 500 um, pore size 400 um, and line height 100 mm. PLA/TCP was deposited into a series of parallel lines along the y direction in the first layer parallel to the x direction in the second layer; the same deposition procedure was applied to the third and fourth layers. The fabrication process produced a solidified PLA/TCP scaffold under normal ambient temperature. The specifications of the materials are indicated in Table 3.

Table 3. 3DP PLA/TCP Composite Scaffolds

	PLA (wt%)	β-TCP (wt%)
PLA	100	0
PLA/TCP30	70	30
PLA/TCP50	50	50
PLA/TCP70	30	70

2. Characterization of 3DP PLA/TCP Scaffold

2.1. Morphological analysis

Scanning electron microscopy(SEM) was performed on a Hitachi Model S3200N SEM. Scaffolds were coated with gold - palladium in a Denton Vacuum evaporator. Images were taken at 70X and 500X.

2.2. Composite characterization

The actual polymer content in the fabricated 3DP PLA/TCP scaffold was measured by thermogravimetric analysis(TGA)(TA Instruments Q5000IR). The samples were heated from room temperature to 120 ℃ at a rate of 20 ℃/min, held for 5 min (to remove absorbed water completely), and heated again to 500 ℃ at the same rate. Polymer weight fraction was normalized to dry sample weight(at 120 ℃). Sample chemical composition was examined by IR spectroscopy(FTIR) using a Fourier Transform Bio-Rad FTS-60V spectrometer that has a scanning range of 500 to 4000cm^{-1} and resolution of 4cm^{-1}. Molecular weight distributions of the composite scaffold were measured using a YL-Clarity GPC system(YL 9170 RI detector) with three columns(Shodex K-802, K-803, and K-804 polystyrene gel columns) at 40 °C. For this measurement, polystyrene calibration was performed and CHCl3 was used as an eluent at a flow rate of 1.0 mL/min. The scaffold fabricated PLA/TCP mixture by freezeer mill was confirmed by X-ray analysis to confirm TCP dispersion within the PLA.

2.3. Mechanical property

Compressive mechanical properties were tested using an Instron 4505 mechanical tester with a 10 KN load cell, following the standard test method for tensile properties (ASTM D638) of plastics.(Fig. 4.) Compressive modulus was calculated as the slope of the initial linear portion of the stress - strain curve. The yield

strength was determined from the cross point of the two tangents on the stress - strain curve around the yield point. All samples were compressed to 50% strain at a speed of 5 mm/min. Statistical results were the average of the five samples.

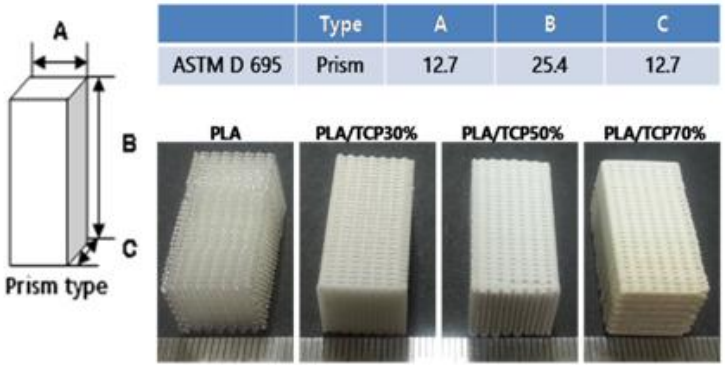

Fig 4. 3DP PLA/TCP composite scaffolds fabricated by using an in 3D plotting system

2.4. Cell proliferation and bioactivity

A mouse osteoblast cell line MC3T3-E1(ATCC) were used in cell seeding experiments. The cell line was cultivated in alpha medium(Gibco™), with the addition of 10% fetal bovine serum(Gibco™), 2% penicillin/streptomycin, and 0.2% Fungizone (GibcoTM) under 5% CO^2 atmosphere at 37°C. MC3T3-E1 cells were seeded on prewetted 3DP PLA/TCP scaffolds of each group at an initial density of 2×10^4 cells/scaffold in 0.2 mL of culture medium and allowed to attach on scaffolds for 3 h in 5% CO2 at 37°C and 95% relative humidity. Cell proliferation was assessed using a nonradioactive water-soluble tetrazolium(WST-8) salt colorimetric assay. The measurement of proliferation was performed after 3, 5 and

7 days. Following the manufacturer's protocol, the scaffold was washed once with phosphate-buffered saline (PBS) then 850 μL fresh culture medium (containing 10% of the WST-8 labeling kit) was added. The cells were incubated for 50 min, and the proliferation rate was measured by monitoring light absorbance at 450 nm using a microplate reader(Biotrak II, UK). Cellular morphology and attachment to the scaffolds were assessed optically using scanning electron microscopy(SEM; Hitachi Model S3200N). MC3T3-E1 cells cultured for 1,3 and 7 days were rinsed with PBS, fixed with 2.5% glutaraldehyde/paraformaldehyde(in PBS) and dehydrated in serials of alcohol dilution of 60 - 100% for 60 min. Later the scaffolds were dried using a critical point dryer(POLARON, UK). The samples were precoated with gold/palladium under an argon atmosphere using a gold sputtering machine(SPI-MODULE™). Later SEM was used to visually explore and observe the cells on all over scaffold surface. Cells were cultivated for up to 14 days in an osteogenic induction medium containing mineralized medium with the addition of 500 μM dexamethasone(Sigma-Aldrich®), 5 mg/mL ascorbic acid (GibcoTM), and 1 M b-glycerolphosphate (Sigma-Aldrich®). Samples were analyzed on culture days 7 and 14. The medium was changed every 36 h. To determine the alkaline phosphatase(ALP) activity, MC3T3-E1 cells were seeded onto 3DP PLA/TCP scaffold in a 12-well culture plate with a density of 25,000 cells/mL and cultured in osteogenesis inducing culture medium. Briefly, 0.1 μM dexamethasone and 10 mM β-glycerophosphate were added to the medium according to Winter et al[19]. β-TCP free PLA scaffold was used as control. The specimens were disinfected before by 70% ethanol for 30 min, washed twice with PBS, and stored in the culture medium or stored for 4 days in PBS (triple exchange) and 1 day in 2 mL cell nutrition medium, respectively. After 7 days and 14 days each of three specimens of each variant were rinsed with tris buffered salt solution (50 mM Tris/HCl pH 7.6, 150 mM NaCl). The cells were resuspended in 1 mL lysis-buffer

[1M diethanolamine/HCl, pH = 9.5, 0.5 mM MgCl2, 0.1% Triton X-100 (w/v)] lysed and kept on ice. Aliquots of 0.1 mL cell lysate and 0.1 mL substrate solution (0.2 mM 4-methylumbelliferylphosphate, 0.5 mM MgCl2, 1M diethanolamine/HCl pH = 9.5) were mixed in cavities of a 96-well microplate (plane bottom) for the subsequent ALP activity measurement. The enzymatic splitting of phosphate was determined by the kinetics of developing fluorescence intensity(excitation/emission at 360/465 nm, multiplate photometer from GeniosPro, Tecan, Germany) each 100 s during 15 min. Relative enzymatic activity was calculated from the linear part of the rising reaction curves. From another aliquot of the lysate, the protein concentration was measured photometrically at 595 nm (by a calibration curve from bovine serum albumine) in the 96-well microplate using the Bradford assay. Thus, it was possible to determine not only the increase of the whole ALP activity but also the amount of protein on the specimens and moreover the AP-activity related to the protein.

3. Effect of in vitro degradation of 3DP PLA/TCP scaffold

3.1. In vitro degradation

In vitro degradation of the 3DP PLA/TCP composite scaffolds was carried out by incubating the samples in phosphate buffered saline (PBS) at 37 ℃ and pH 7.4 for 8 weeks. The incubation medium was replaced by the fresh PBS solution weekly. The pH value of the PBS solution during degradation was monitored by a pH meter(Mettler Toledo 320 pH meter). Six paralleled scaffolds of each degradation conditions were taken out every two week, washed with distilled water and vacuum-dried for further characterizations.

3.2 Characterizations

A. Water absorption

Scaffolds were taken out from PBS solution at intervals and weighed by an electrical balance with a resolution of 0.1 mg after wiping off the surface water to obtain the wet mass, m_t,w. Scaffolds were then washed with distilled water and dried in vacuum for 24 h. The dried mass was characterized as m_t. Water absorption of the scaffolds was calculated by the following equation:

$$\text{Water absorption} = (m\text{t,w} - m_t)/m_t \times 100\%$$

B. Morphology

Samples before and after degradation were fractured after frozen in liquid nitrogen for 30 min. The fractured section was observed under a Philips XL30 scanning electron microscope(SEM) after gold coating.

4. In vivo investigations on 3DP PLA/TCP composite scaffold

4.1. Rat calvarial defect model

A. Surgery and transplantation procedure

Forty eight SD male rat with a body weight of 190 - 200 g were used as transplant recipients. Before surgery, the animals were kept in clean and standard air conditions at a constant temperature of 21 ℃. Rats were anesthetized by intramuscular injection of 50 mg/kg ketamine hydrochloride with 5 mg/kg diazepam under sterile conditions. Then, skin and periosteum were raised to expose the calvaria. In all of the rats, an 8 mm critical-size defect was made in the rat calvarial bone by a trephine burr. Constant saline irrigation was provided

and the dura mater was kept intact. The procedure was performed under sterile conditions. After transplantation, the skin incision was closed with nylon sutures. The animals were kept in sterile condition with enough water and foods.(Fig. 5.)

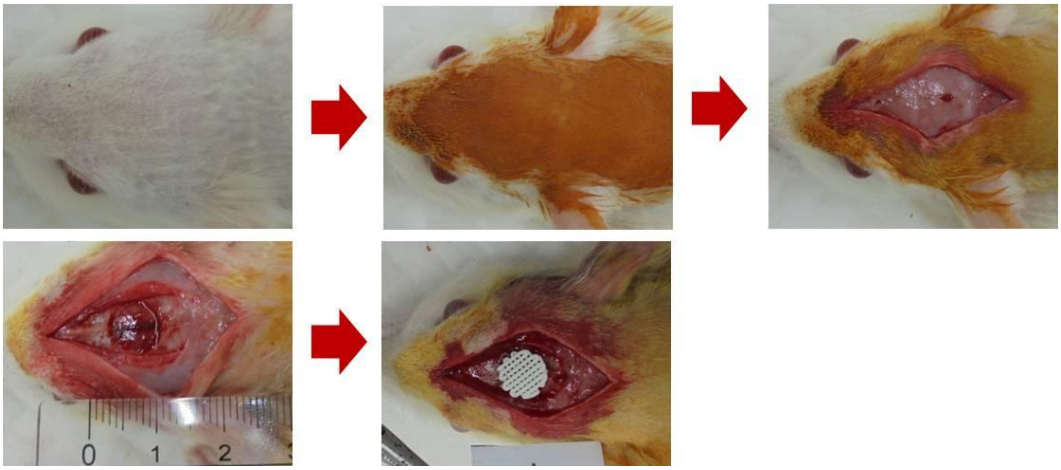

Fig 5. Rat calvarial defect model. Surgical procedures of rat 8 mm diameter calvarial defect using trephine bur.

In all of 48 calvarial bone defects were randomly divided into four groups: control group with empty defect, first experimental group defect filled with 3DP PLA (50% β-TCP), second experimental group defect filled with 3DP PLA/TCP (70% β-TCP), third experimental group defect filled with 100% β-TCP. The rats were sacrificed 2, 4 and 8 weeks after transplantation and their calvarial with grafts were harvested.

B. Micro computed tomography (Micro-CT) analysis

All the rats were sacrificed by an intraperitoneally overdose injection of pentobarbital. Then the calvarial bone was explanted and fixed in 4% phosphate-buffered formalin solution. The new bone formed in the calvarial bone defect was assessed using a Micro-CT system (lCT-80, Scanco Medical, Switzerland). The CT settings were used as follows: pixel matrix, 1, 024×1,024; pixel size, 20 um; slice thickness.. After tomographic acquisitions, 2D cross-sectional scanning slices of the 5 mm calvarial bone defects area and surrounding tissue were reconstructed using Mimics software (Materialize, NV, Leuven, Belgium) and 3D images were displayed in Geomagic studio 11.0 software (Geomagic (Shanghai) Software Co., Ltd, USA)

C. Histological analysis

After retrieval of the samples, they were fixed in 10% fomalin for 48 h, rinsed with PBS several times, embedded in OCT (KMA-0100-00A, CellPath Ltd., UK), and sectioned (10-mm thick). Before embedding in OCT, the calvarial bone was decalcified by treating it with Decalcifying Solution-Lite(D 0818, Sigma Aldrich, USA). Representative sections were stained with H&E, Masson's trichrome and visualized using an optical microscope.

4.2. Rabbit osteochondral defect model

A. Surgery and transplantation procedure

Thirty-six, 9-month-old New Zealand white rabbits, weighing more than 4kg were used in this study. All surgical procedures followed protocols based on a well-established bilateral, rabbit, osteochondral defect model.[87-89] Both knees in each rabbit underwent surgery under sterile conditions. In total 72 knees were randomly assigned into three groups, including empty defect (n = 8 knees), 3DP

PLA/TCP70 (70% β-TCP) (n = 8 knees) and β-TCP(100%) (n = 6 knees).(Fig. 6)

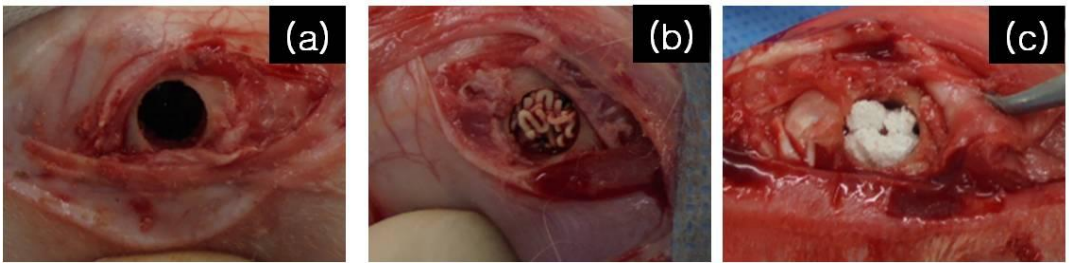

Fig 6. Experimental design. The defect were kept empty(a); filled with 3DP PLA/TCP70 scaffold(b); β-TCP powder was implanted(c)

Twelve rabbits were used to examine tissue repair at 4 weeks, with the remaining twenty-four rabbits utilized to examine repair at 8 and 12 weeks Prior to surgery, anesthesia was induced by an intravenous injection of Hypnorm(0.32 mg/mL fentanyl citrate and 10 mg/mL fluanisone) and atropine. General inhalation anesthesia was then maintained by a mixture of nitrous oxide, isoflurane, and oxygen administered through a constant volume ventilator. To reduce peri-operative infection risk and to minimize postoperative discomfort, antibiotic prophylaxis (Baytril 2.5%, Enrofloxacin, 5 - 10 mg/kg) and Fynadynewere preoperatively administered to the rabbits. After administration of anesthesia, rabbits were immobilized on their back. Hair from both legs of each animal was shaved, and the legs disinfected with povodine - iodine. Both knee joints were then exposed through a medial parapatellar longitudinal incision. The capsule was incised, and the medial femoral condyle exposed after lateral luxation of the patella. With the knee maximally flexed, a full-thickness defect (6 mm in diameter and 10 mm in depth) was created in the center of the condyle using a dental drill (KAVO, Intrasept 905, KAVO Nederland BV, Vianen, The Netherlands). A 2-mm

drill bit was first used to establish a 2-mm diameter defect. This defect was then irrigated and gradually enlarged using drill bits with a diameter of 2.8 mm and then 6.0 mm. All bits were fashioned with a 10 mm stop to ensure a defect of precisely 10 mm in depth was created. All debris was removed from the defect with a curette and the edge carefully cleaned with a scalpel blade A 3DP PLA/TCP70(3 mm in diameter and 2 mm in height) scaffold and β-TCP powder was then placed into the defect. Subsequently, the patella was repositioned, and the capsule and muscle closed with a continuous 4-0 Vicryl suture. Finally, the skin was closed with single intracutaneous 4-0 Vicryl sutures.(Fig. 7) This procedure was repeated for both knees of each rabbit with different scaffold formulations implanted into the right and left knees of each rabbit. To minimize postoperative discomfort, Fynadyne was administered for 2 days postoperatively. The animals were housed in conventional rabbit cages that allowed for unrestricted weight-bearing activity and were observed for signs of pain, infection, and proper activity.

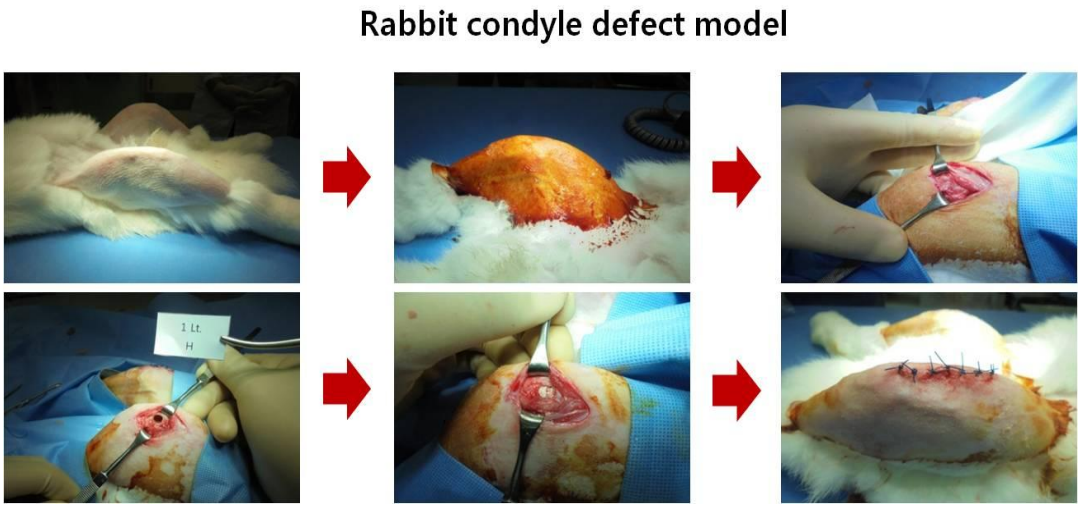

Fig 7. Rabbit osteochondral defect model. Intraoperative pictures of defect preparation.

B. 3D-Bone analysis for bone mineral density (BMD) and bone quantity (BV/TV)

To obtain a quantitative measure of the regenerated bone, microtomograph (Skyscan, 1076 scanner) imaging was performed on the experimental and control rabbit medial femoral condyles. The dissected, formalin-fixed rabbit femur ends were placed on a sample holder with the femur axis perpendicular to the plane of scanning. Samples were scanned through a 180° rotation angle with a rotation step of 0.8° at 35 μm resolution. The image data was reconstructed and Mimics (Materialize, Belgium) was used to visualize the 3D representation of the regenerated bone. From the CT data set, a cylindrical region of interest (ROI) was selected for analysis. This ROI corresponds to the original defect location. To evaluate the topographic bone regeneration level within the defect, the ROI was sectioned transversely as top, medium and bottom sections and radially as outer, inner shells and core. Seventy-two femoral medial condyles from age-matched un-operated rabbits were used as controls. The degree of bone regeneration occurring within the osteochondral defect was presented as a percentage of the native bone volume fraction.

III. RESULTS

1. Characterization of 3DP PLA/TCP Scaffold

1.1. Morphological analysis

The fabricated disk-shaped scaffolds conformed to the target specifications of diameter of 8 mm, line width of 500 um, line gap of 400 mm, and had fully-interconnected pores (Fig. 8).

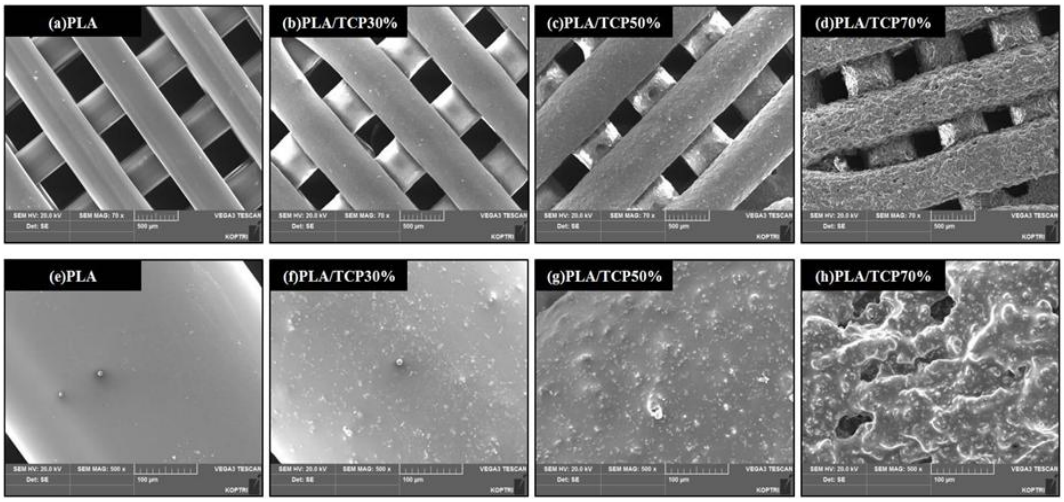

Fig. 8. SEM images of 3DP PLA/TCP composite scaffold with increasing TCP content (a,e: 0 wt% TCP ; b,f: 30 wt% TCP; c,g: 50 wt% TCP; and D,H: 70 wt% TCP).

The interconnected porosity has a vital function in the transportation of nutrients and oxygen, and in removal of waste. The generated line width of ~500 um and pore size of ~400 um, are appropriate for bone tissue engineering scaffolds. This kind of microperiodic architecture has been shown to be effective for bone regeneration in vivo. The surface of the PLA scaffolds was smooth, whereas that of the PLA/TCP with various content of β-TCP was rough due to the included TCP powder(Fig 8. f, g, h). The surface roughness enhances cell attachment and thus 3DP PLA/TCP scaffold should do so.

2. Composite characterization

2.1 TGA analysis

Thermogravimetric analysis (TGA) was used for analytic measurement of component ratios of polylactide and calcium phosphate. According to TGA measurements, Fig. 9, the actual polymer contents of 3DP PLA/TCP30%, PLA/TCP50% and PLA/TCP70% nanocomposites (31.37, 51.25 and 67.57 % by weight, respectively) closely correspond to the nominal values. This suggests that no PLA was lost in the course of nanocomposite powder synthesis and high pressure consolidation.

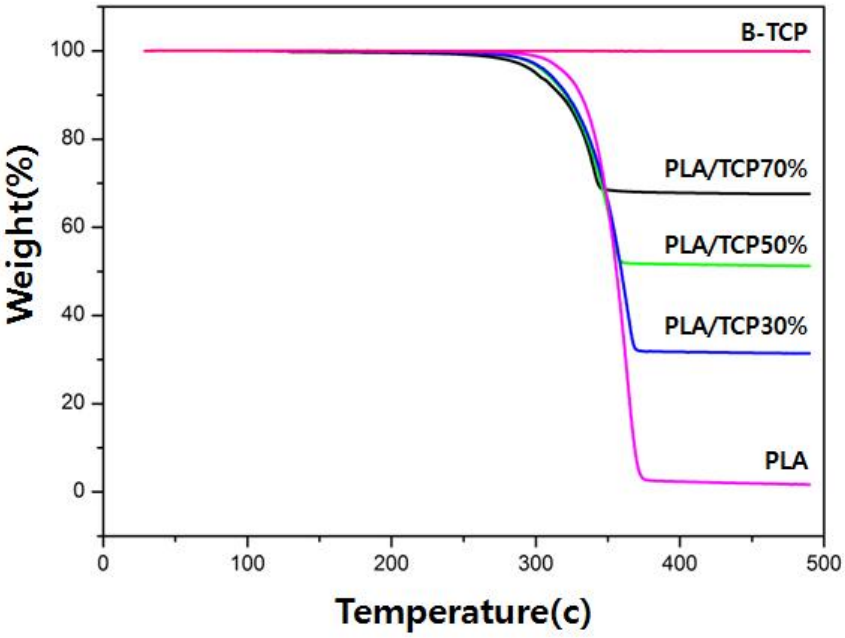

Fig 9. TGA curves for pure β-TCP and for 3DP PLA/TCP composite scaffolds containing 30, 50 and 70% polymer

2.2 FT-IR

FT-IR analyses with the functional organic groups in the polymers and in the β-TCP are shown in Fig 10. In the case of the PLA, it is known that the absorbance at 1756.0 cm−1 corresponds to carbonyl stretching and, at 1185.0 and 1087.0 cm^{-1} to stretching vibrations of the C\O\C groups. Also, it can be seen absorption peaks of PO_4^{3-} at 615 and 557 cm^{-1} which are attributed to β-TCP. In all spectra, except for PLA raw material and 3DP PLA scaffold, the range of 557~615cm^{-1} exhibits a typical absorption band related to PO_4^{3-}. It's an indicative of incorporation of the β-TCP in the 3DP PLA/TCP scaffold, showing that a physical interaction between them occurred.

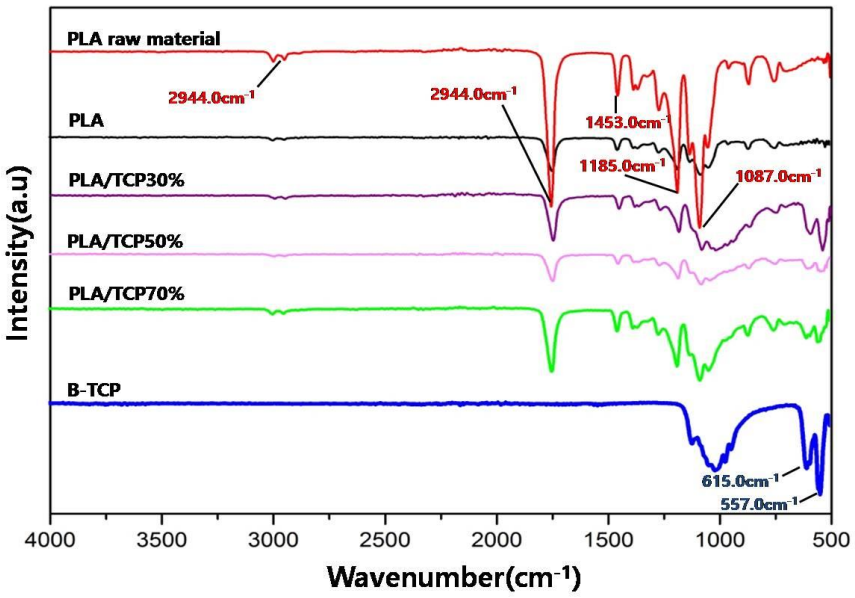

Fig. 10. FT-IR spectra of: PLA Raw material, 3DP PLA scaffold(PLA), 3DP PLA/TCP with different contents β-TCP(30%, 50% and 70%) and β-TCP raw material.

2.3 GPC

The molecular weight and molecular weight distribution of the 3DP PLA/TCP scaffold were determined by GPC measurement and the results are shown in Table 3. It could be seen that with increasing degradation time both weight average molecular weight (Mw) and number average molecular weight (Mn) of the remaining PLA decrease (as shown in Table. 4).

Table 4. The effect of the 3D plotting system and the presence of β-TCP on 3DP PLA/TCP svaffold molecular parameters Mn and Mw measured by GPC in chloroform

	Mn	Mw	Mp	Mw/Mn
PLA raw material	52,800	205,000	197,000	3.89
PLA	29,200	104,000	79,900	3.55
PLA/TCP30%	19,600	54,700	46,800	2.71
PLA/TCP50%	18,200	47,200	44,400	2.59
PLA/TCP70%	19,000	51,500	46,300	2.7

2.4 Compressive mechanical properties

Bone tissue engineering scaffolds should have sufficient mechanical strength for bone regeneration at the site of implantation and maintain structural integrity during both in vitro and in vivo cell growth. Different concentrations of β-TCP nanoparticles were added to 3DP PLA/TCP scaffold and the compressive modulus was measured. The compressive modulus of the 3DP PLA/TCP scaffolds decresed with increasing β-TCP concentration(Fig 11). The compressive modulus of the 3DP PLA scaffolds was 38 MPa, while the compressive modulus of the 3DP PLA/TCP 70% scaffold was 5 MPa. This decreased modulus indicated that incorporation of β-TCP nanoparticles in the 3DP PLA/TCP scaffld undermined mechanical properties due to particle enhancement.

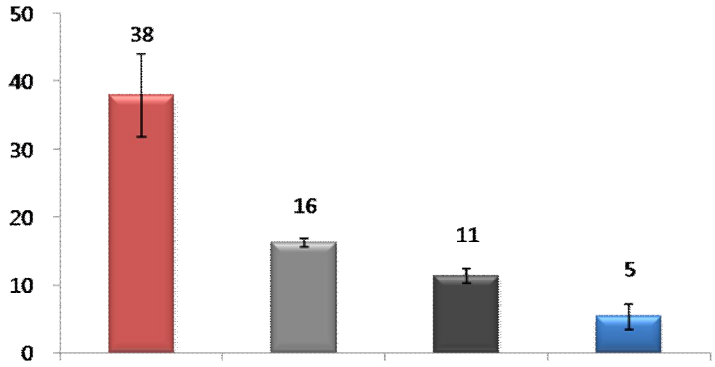

Fig. 11. Characterization of the compressive strength of the scaffolds.

2.5 Optimization of β-TCP powder dispersion

The β-TCP powder distribution is critical for enabling a well-packed, smooth powder bed for printing and also for dictating the intrinsic micro-porosity and resolution of the printed material. Therefore, the TCP powder was grinded and mixed with PLA powder by freezer mill. Then the mixture was collected from between two stainless steel meshes (ranging 30 - 150 μm) to remove particulate that was too large for accurate printing and too small to avoid agglomeration. The prepared mixture was placed in a 50 mL steel syringe fastened to the 3D plotter, and dispensed through a steel nozzle at temperature >180 ℃ by applying a pneumatic pressure of 600 kPa; the feed rate was 100 mm/min. The dispersion of TCP powder was confirmed within PLA/TCP scaffold by X-ray analysis, whereas PLA/TCP mixture without freezer mill process was not printed.(Fig. 12.)

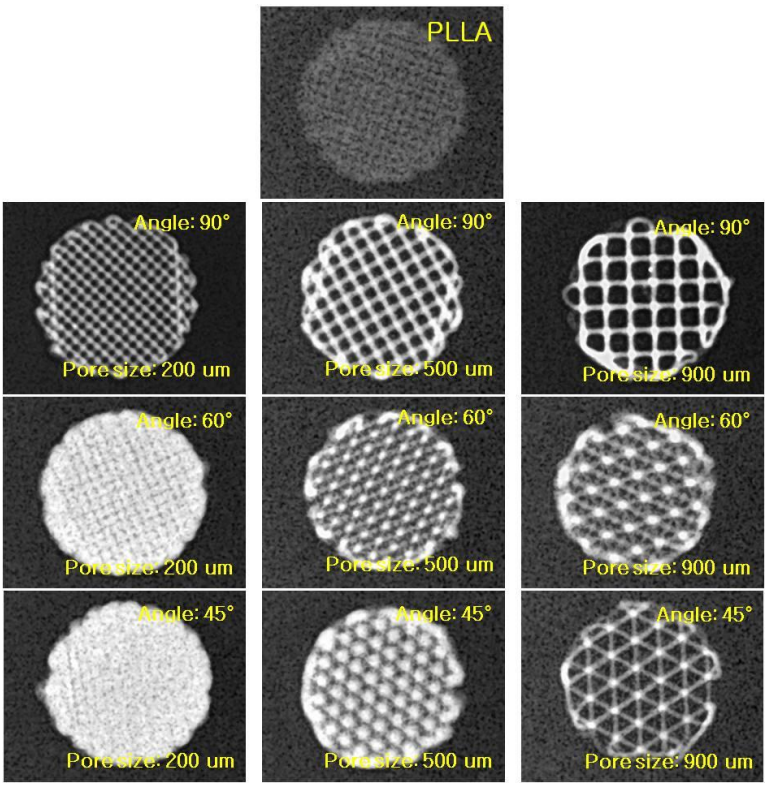

Fig. 12. Characterization of the β-TCP powder dispersion

2.6 Cell proliferation and bioactivity

A. Cell Proliferation

Proliferation of cells continuously increased from culture day 3 to culture day 7 among all groups. On culture day 3, PLA/TCP50 and PLA/TCP70 scaffolds showed significantly higher cell numbers than the PLA scaffold, whereas PLA/TCP30 behaved similar to the pure group. On culture day 5 and 7, all groups showed significantly higher cell numbers than the PLA scaffold, The proliferation of cells on PLA/TCP70 were higher than other ratios. (Figure 13)

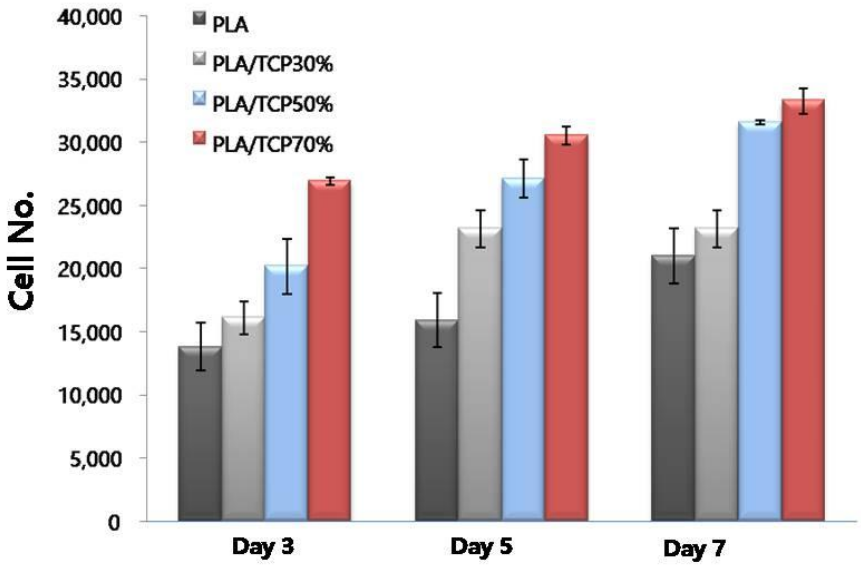

Fig. 13. Cell number among different ratios as revealed by WST-8 assay during culture days 3, 5, and 7.

B. ALP activity

PLA/TCP50 and PLA/TCP70 Scaffold increase in ALP activity from culture days 7 to 14, but there were no significant increase and differences in PLA and PLA/TCP30. Later on, On culture day 14, PLA/TCP70 showed a significant higher ALP activity than other group.(Fig. 14.)

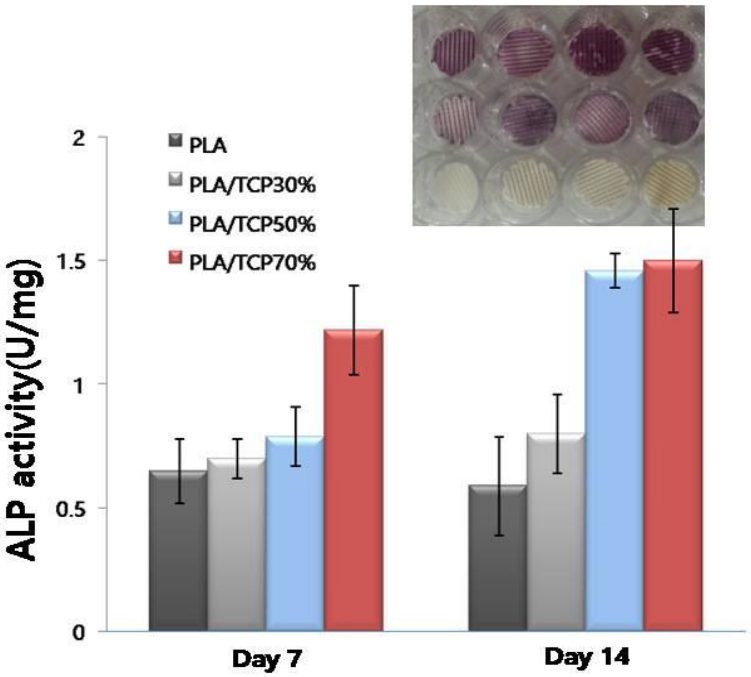

Fig. 14. ALP activity among different ratios during culture period.

C. Cell morphology

MC3T3 cells were cultured on the 3DP PLA/TCP scaffold for 24 h and analyzed with SEM that showed the ability to interact with 3DP PLA and all 3DP PLA/TCP scaffold. It was observed that for all compositions, cells were attached at the scaffolds surface; however, cell adhesion was more significant in the scaffolds with 10% of CNT. In that case, the cell number attached to the surface was bigger during all the culture periods, and at the 6th day of culture, the material is already covered with a cellular layer. The cells presented a typical elongated morphology, with cytoplasmatic extensions and intercellular connection as it can be seen in Fig 15. These data confirm that the higher the amount of TCP, the better is cell adhesion and cell spreading.

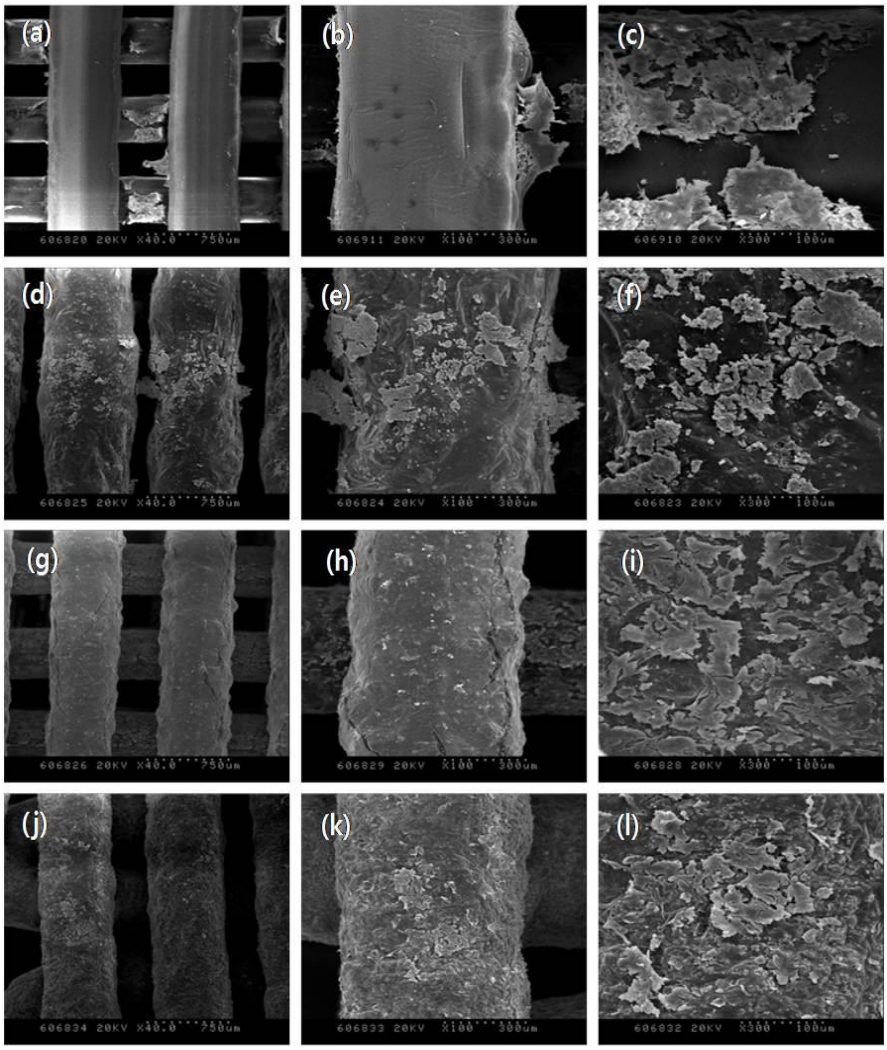

Fig. 15. SEM images of MT3T3 cell on the 3DP PLA/TCP scaffold, (a), (b), 3DP PLA scaffold; (d), (e), (f) 3DP PLA/TCP 30%; (g), (h), (i) 3DP PLA/TCP 50%; and (j), (k), (l) 3DP PLA/TCP 70%.

3. Effect of in vitro degradation of 3DP PLA/TCP scaffold

3.1. In vitro degradation

A. pH change

Figure 16 illustrates the pH change of PBS solution over time. None of the groups showed significant pH changes until week 2 with a pH value between 7.08 - 7.11. The pH of each group decreased between weeks 2 and 4. PLA/TCP50% and PLA/TCP70% pH normalized in a range of 7.24 - 7.27 throughout the experiment, while PLA and PLA/TCP30% scaffolds decreased pH at week 8.

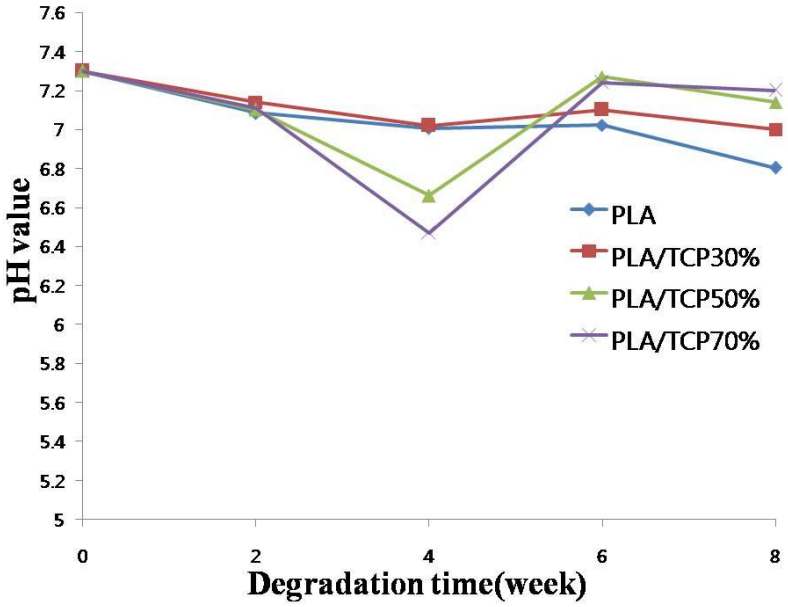

Fig. 16. Changes in pH of PBS solution used for in vitro degradation of composite scaffolds at 37°C

B. Water Absorption

Water absorption changes of composite scaffolds during degradation are shown in Fig 17. Results suggested that the water absorption increased sharply in the first 2 weeks and went up to a saturated plateau. The water absorption of the PLA/TCP50% and PLA/TCP70% after degradation remained higher than PLA and PLA/TCP30% in the first 2 weeks, and became lower later. The water absorption process is a balance between the dissolution of oligomers in the solution and water uptake of the residual material. An increase in water absorption reflected the extent of PLA degradation in the initial stage. Accumulation of the hydrophilic degradation products inside the scaffolds resulted in the increase of water absorption during the whole degradation process.

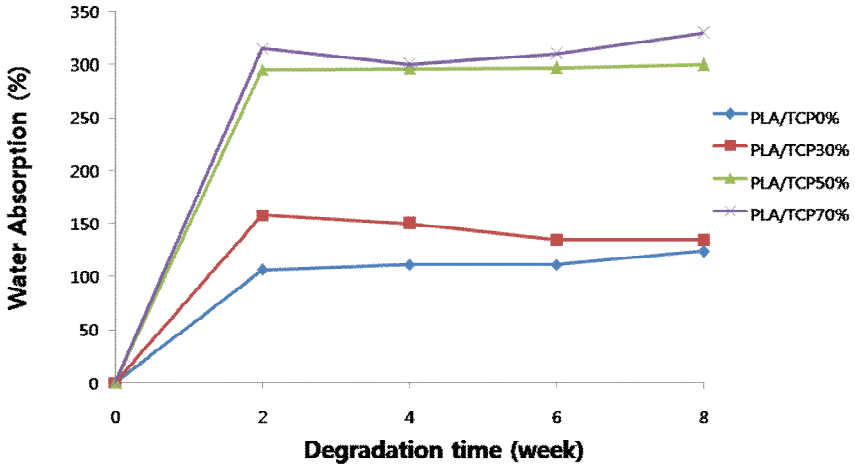

Fig. 17. Water absorption changes of the 3DP PLA/TCP composite scaffolds during degradation.

C. Morphology

Fig. 18 shows morphology changes of the PLA/TCP composite scaffolds before and after degradation . Results suggested that the wall of the scaffold before degradation was smooth in an inorganic - organic continuity. After degrading for 4 weeks, some pores could be seen on the wall of the scaffolds. When the scaffolds were degraded for 6 and 8 weeks, more TCP particles and more pores were observed on the wall. Also showed some cracks on the wall of the scaffolds after 8 weeks of degradation under dynamic conditions. In contrast, the composite scaffolds still exhibited a fairly smooth surface in a good organic-inorganic continuity under static conditions after degradation for the same time.

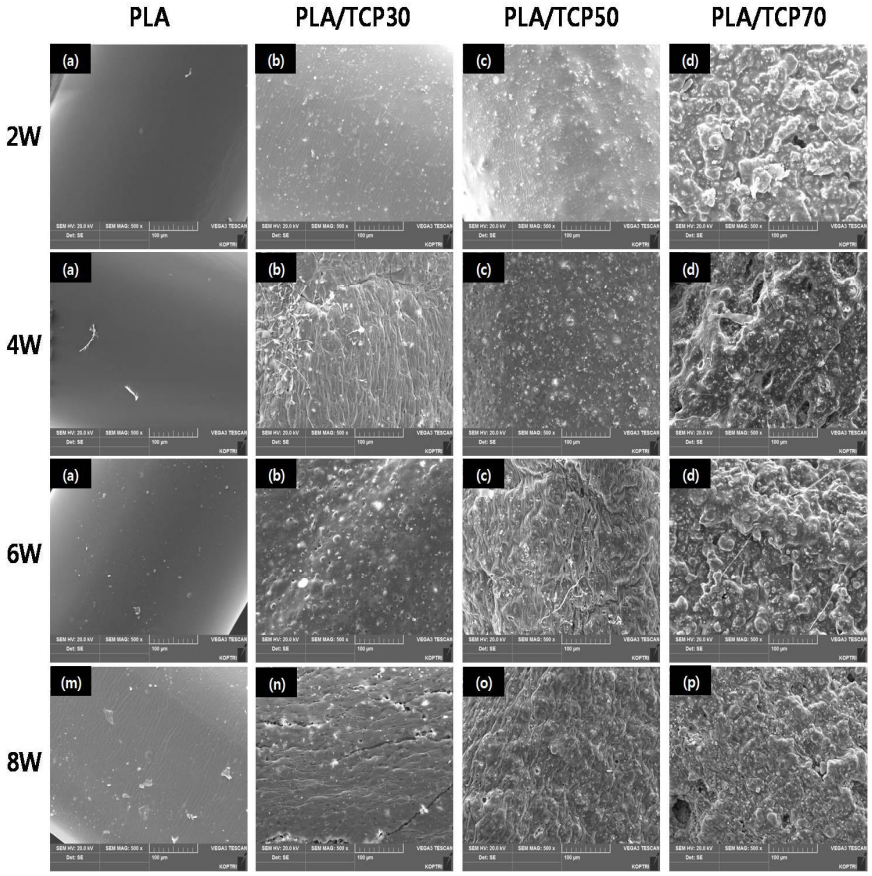

Fig. 18. SEM micrographs of 3DP PLA/TCP scaffolds after degradation for 2 (b,c), 4 (d,e) , 6 and 8 weeks (f,g), respectively.

4. In vivo test

4.1. Rat calvarial defect model

A. 3D-Bone analysis for bone mineral density (BMD) and bone quantity (BV/TV)

The results from the Micro CT analysis of the explanted defects 2, 4, and 8 weeks post-implantation are shown in Fig. 19. The Micro CT images show that there was no de novo bone tissue within the defects that were untreated. 3DP PLA/TCP50, PLA/TCP70 and TCP100 scaffolds were able to elicit a certain level of tissue healing as demonstrated by new regions of bone within the defect. Importantly, the defect was completely filled with new bone in the animals where a 3DP PLA/TCP70 scaffold was implanted; additionally, there were no signs of either bone anomalies or bone resorption on defect adjacent areas. The total volume of newly formed bone within the ROI was measured by assigning a threshold for total bone content (including trabecular and cortical ranges) and subtracting any contribution from the scaffold (determined previously).The bone volume was 12.66 (±2.51), 24..66 (±2.51) and 26.33(±3.05) at 2, 4 and 8 weeks, respectively, in the control group; 41.66 (±1.05), 40.42 (±5.03) and 48.07(±1.72) at 2, 4 and 8 weeks, respectively, in the PLA/TCP50 group; and 44.33 (±1.66) and 47.41 (±0.85) and 55.64(±3.06) at 2, 4 and 8 weeks, respectively, in the PLA/TCP70 group; and 27.9 (±2.61), 33.66 (±1.65) and 37.37 (±2.0) at 2, 4 and 8 weeks, respectively, in the TCP100 group. The PLA/TCP50 and PLA/TCP70 groups had significantly greater neo-tissue areas than did the control and TCP100.(Fig. 20)

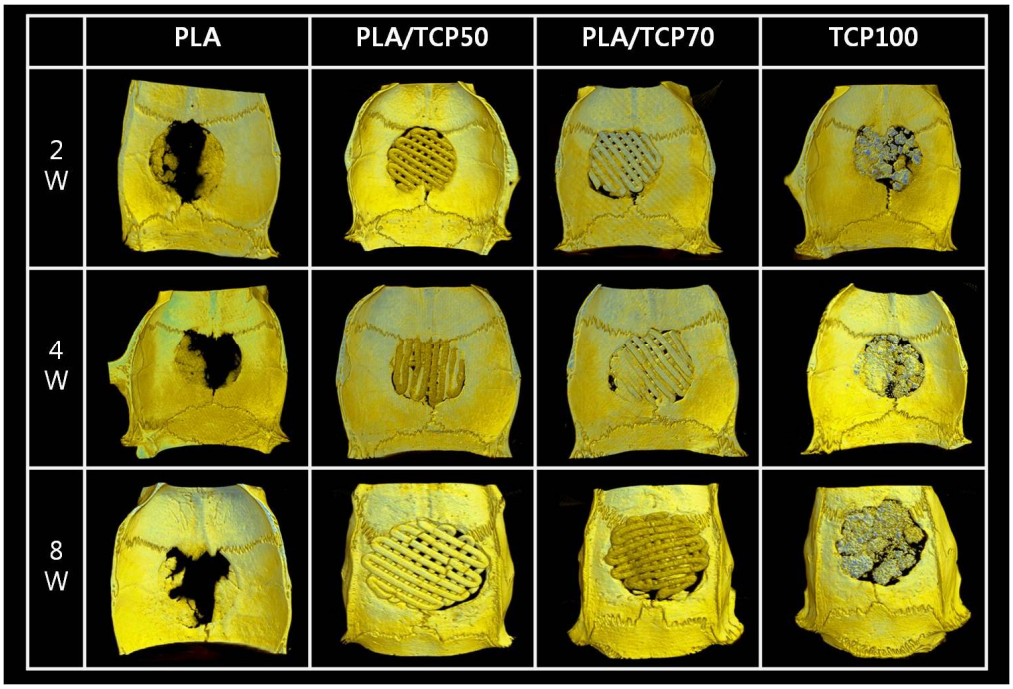

Fig. 19. 3D micro-CT images in each group, the PLA/TCP50 and PLA/TCP70 group had significantly greater neo-tissue area than the TCP100 group at 4 and 8 week.

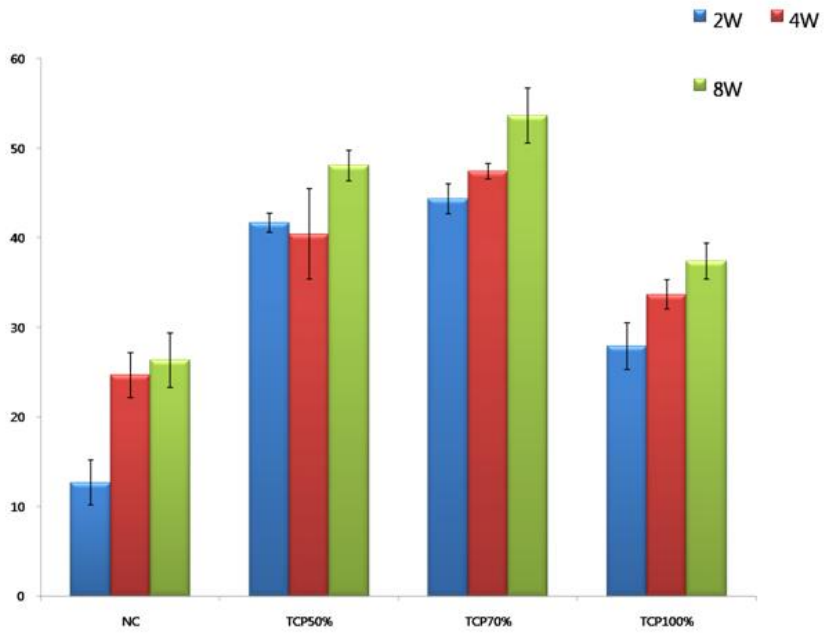

Fig. 20. New bone volume in rat calvarial

B. Histological analysis

Several different stains can be applied to the histological sections of the defect. Hematoxylin and eosin is a general stain used to highlight cellular components, where the nuclei of cells are stained blue and the cytoplasm is stained pink. Representative H&E staining showed enhanced bone formation in the 3DP PLA/TCP70 scaffolds, compared with the 3DP PLA/TCP50 and TCP100 scaffolds, at 4 and 8 weeks after implantation. Eight weeks post implantation, new bone formation and bridging of the defect occurred predominantly in the PLA/TCP70 scaffold.(Fig. 21).

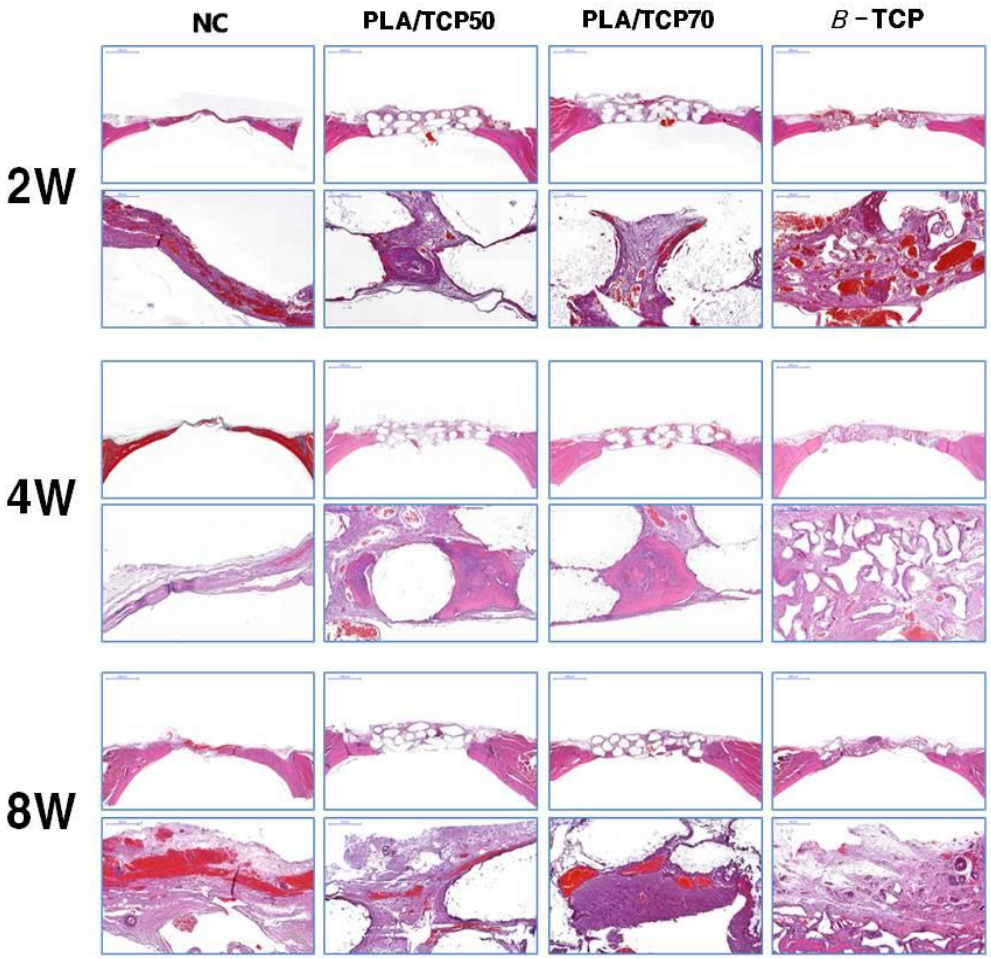

Fig. 21. H&E-stained sections of rat calvarial defects implanted with PLA/TCP50, PLA/TCP70 and β-TCP at 2, 4 and 8 weeks

Decalcified sections were stained with Masson's Trichrome to identify new bone formation and osteoid within the healing defects. From all perspectives it is quite clear that bone healing was markedly better within 3DP PLA/TCP70 scaffolds. Bone formation was minimal within empty defects, commencing only from the periphery of host bone for the all of scaffolds, but nearly filling the defects when 3DP PLA/TCP70 was implanted at 8 weeks. Staining for collagen with picrosirius red showed the PLA/TCP scaffolds to have the most robust and uniform distribution of collagen. Evaluation with polarized light showed the greatest amount of type I collagen in the PLA/TCP70 constructs.(Fig. 22)

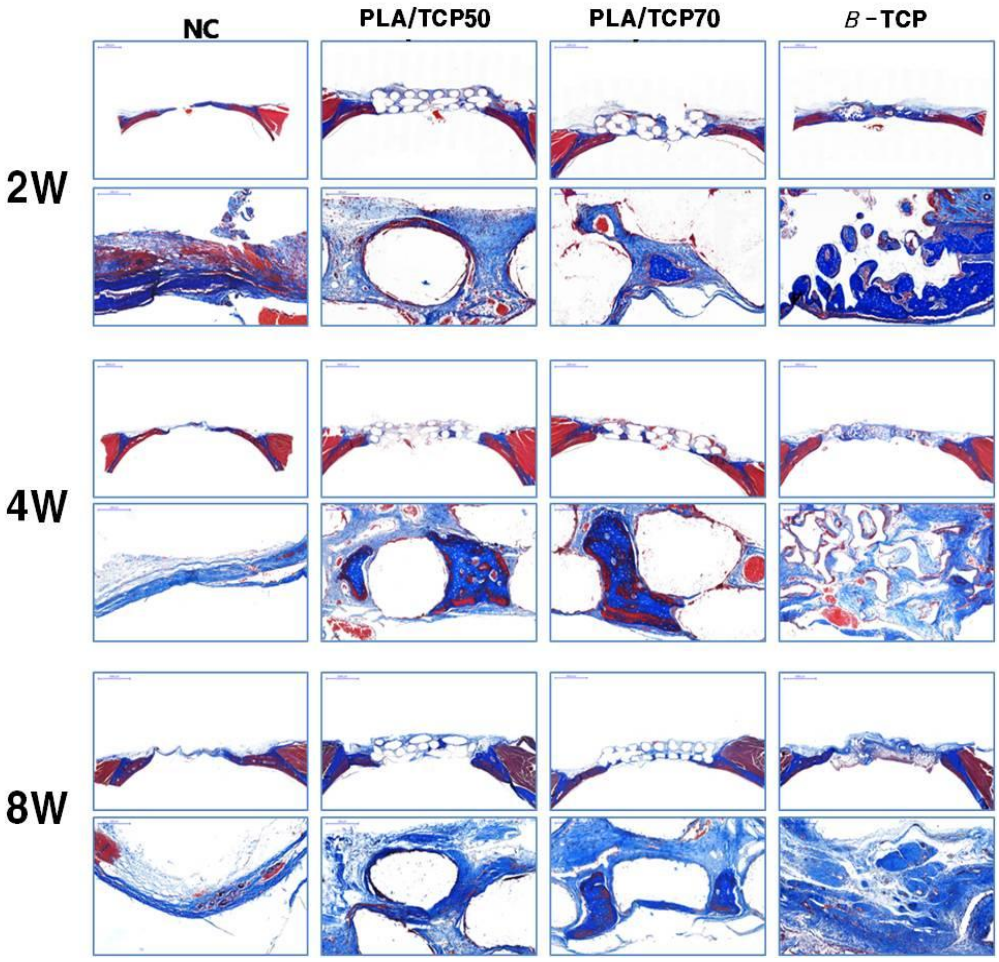

Fig. 22. Masson's Trichrome stained sections of rat calvarial defects implanted with PLA/TCP50, PLA/TCP70 and β-TCP at 2, 4 and 8 weeks

Goldner's trichrome is to show mineralized and nonmineralized osteoid seen in blue/green or red, respectively. Figure 21 shows mineralized and nonmineralized osteoid within the pores of the scaffold. Bone formation area, as evaluated by histomorphometry, was much larger in the implants of 3DP PLA/TCP50 and 3DP PLA/TCP70 scaffolds than β-TCP (Fig. 8d). Inflammation was not observed in the histological sections at calvarial defect site. (Fig. 23).

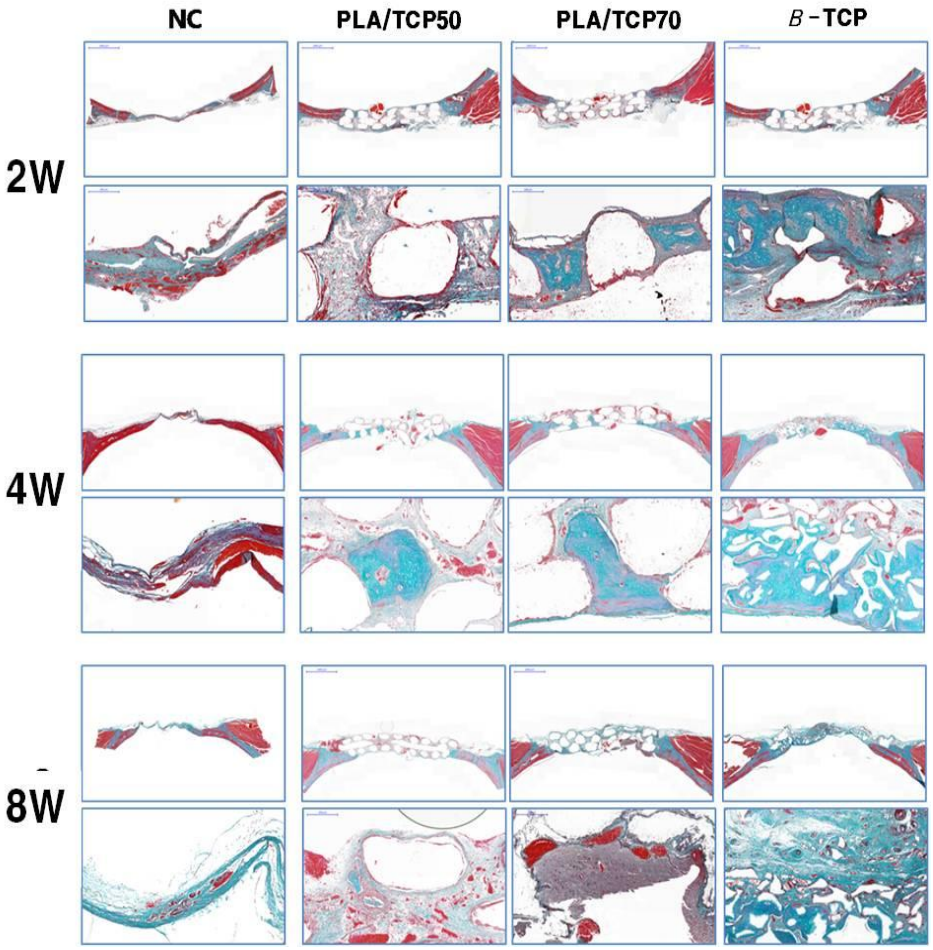

Fig. 23. Goldner's trichrome staining of rat calvarial defects implanted with PLA/TCP50, PLA/TCP70 and β-TCP at 2, 4 and 8 weeks

4.2. Rabbit osteochondral defect model

A. 3D-Bone analysis for bone mineral density (BMD) and bone quantity (BV/TV)

The regenerated osteochondral bone was evaluated using micro-CT images in sagittal planes that passed through the center of the defect(Fig. 24). Bone formation in the defect group was very poor up to 12 weeks after the operation. The subchondral bone defects in the groups that received all of implants began to exhibit signs of restoration at 8 weeks. Although the bone restoration in the β-TCP were moderate thereafter, the defect was completely filled with new bone in the animals where a 3DP PLA/TCP70 scaffold was implanted; additionally, there were no signs of either bone anomalies or bone resorption on defect adjacent areas.

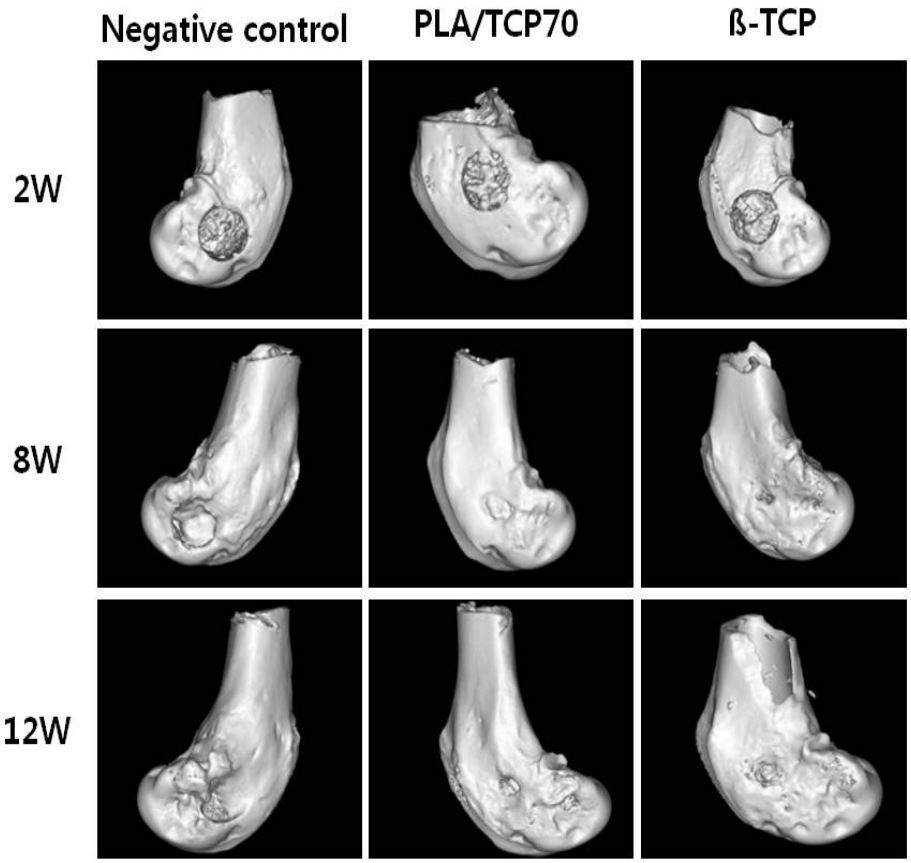

Fig. 24. 3D Micro-CT images in osteochondral defect, the PLA/TCP70 and β-TCP group.

Quantitative analysis of regenerated osteochondral bone (Table. 5) showed that, in comparison to the defect group, significantly more osteochondral bone bone was formed in the three groups that were implanted with PLA/TCP70. In particular, the bone volume in the PLA/TCP70 group was greater than β-TCP at 12 weeks.

Table 5. New bone volume in rabbit osteochondral bone

Time after implantation(weeks)	Bone volume(mm^3)		
	Negative control	PLA/TCP70	β-TCP
2	0.13±0.07	3.6±0.12	2.9±0.19
8	2.30±0.31	8.25±0.9	6.39±1.26
12	3.01±0..22	25.64±3.52	16.54±2.32

IV. DISCUSSION

The use of engineered polymer scaffolds as structural bone substitutes offers a promising alternative to biological allografts. Scaffolds can be engineered to tune their chemistry and microarchitecture to optimize delivery of cells and osteogenic factors as well as to enhance their mechanical properties. The success of a scaffold as a structural bone substitute depends on achieving and maintaining a balance between the biological and mechanical (functional) requirements, both of which depend on scaffold's porosity. The 3D printing method can be used to fabricate a customized and solvent-free scaffold with tailed bone geometry and interconnected pore structures for repair of bone defects. In this study, a commercial 3D printer and freezer mill was adapted to create composite bone graft substitutes for tissue engineering applications and preclinical studies of bone healing in animal models. The PLA and β-TCP was used in this study, that's because the β-TCP and PLA are respectively alkaline degradation products and acidic degradation products, the neutralization of them can break the PLA autocatalytic reaction cycle chain, which can reduce early degradation ratio. In addition, another important reason for selecting this material is that it can reduce the incidence of aseptic inflammation, which can create a favorable microenvironment for the osteoblast proliferation and new bone formation. While other studies have investigated parameters related to the β-TCP powder, such as chemical composition and particle size, the current study focused on enhancing 3D printed polymer/ceramic composite. The primary advantages of 3D printing and freezer mill in biomaterials applications is to enhance β-TCP contents. In the previous study, content of β-TCP did not exceed 50% because of viscosity their PLA/TCP composit. The current study confirms the benefits of freezer mill for improving the printability of the PLA/TCP composit added 70% β-TCP, which enhanced the osteogenesis and biocompatibility. This study showed that adding

increasing contents β-TCP to a lactic acid polymer matrix stimulated the proliferation of MC3T3-E1(ATCC) cells and synthesis of the extracellular bone matrix in a dosedependent manner. In vivo results indicate that, in comparison with pure β-TCP, β-TCP containing composite materials had faster degradation kinetics, caused less inflammatory reaction, and promoted contact osteogenesis. The composite material containing 70% β-TCP demonstrated a improve performance to pure TCP bone grafts in terms of osteogenesis, and is apparently compatible with the production of intra-osseous implants for obtaining bone fusion or healing. Further studies are necessary to evaluate the ability of such a composite material to retain sufficient mechanical strength overtime for providing safe correction or stabilization of the implanted bone fragments.

V. CONCLUSION

This study demonstrates strategies for 3D printing technology and optimization of material parameters to fabricate PLA/TCP composit material for applications of bone regeneration. These scaffolds are printed with 70% β-TCP contents to achieve improvement of osteogenesis. PLA/TCP composit scaffold include macropores and have microporosity that is critical for fluid exchange and cellular influx during bone healing. The materials are sufficiently strong for handling and placement into a non-loading bone defect and are degradable and osteoconductive, which allows replacement and incorporation of these scaffolds into the newly forming bone.

REFERENCE

1. Jeffrey B Kerr (2000) Atlas of Functional Histology , Mosby, USA

2. Karin A. Hing. Bone repair in the twenty-first century: biology, chemistry or engineering? Philosophical Transactions of the Royal Society A:Mathematical, Physical and Engineering Sciences 362, 2821-2850. 2004.

3. Alexander P. Spence (1986) Basic Human Anatomy, Benjamin-Cummings, USA

4. Jeffrey B Kerr (2000) Atlas of Functional Histology , Mosby, USA

5. Riminucci, M. and Bianco, P. (2003) Building bone tissue: matrices and scaffolds in physiology and biotechnology. Braz J Med Biol Res 36, 1027-36.

6. Dale Layman (2004) Physiology demystified, McGraw-Hill, USA

7. Hong, Sun, Hong, Soon, and Kohn, David. Nanostructural analysis of trabecular bone. 20(7), 1419-1426. 2009-.

8. Margareta Nordin and Victor H.Frankel (1989) Basic Biomechanics of the Musculoskeletal system, Williams & Wilkins, USA

9. Liebschner, Michael A. K. Biomechanical considerations of animal models used in tissue engineering of bone: Animal Models for Tissue Engineering Applications. Biomaterials 25(9), 1697-1714. 2004.

10. Hamer, A. J., Colwell, A., and Eastell, R. Biomechanical and biochemicalchanges in cortical allograft bone after gamma irradiation. Bone 19(6), 696. 96.

11. Hamer, A. J., Colwell, A., and Eastell, R. Biomechanical and biochemicalchanges in cortical allograft bone after gamma irradiation. Bone 19(6), 696. 96.

12. Mroz, Thomas E., Lin, Eric L., Summit, Matthew C., Bianchi, John R.,Keesling, Jr. Jim E., Roberts, Michael, Vangsness, Jr. C. Thomas, and Wang, Jeffrey C. Biomechanical analysis of allograft bone treated with a novel tissue sterilization process. The Spine Journal 6(1), 34-39. 2006.

13. Liebschner, Michael A. K. Biomechanical considerations of animal models used in tissue engineering of bone. Biomaterials 25(9), 1697-1714. 2004.

14. Xiaodu Wang and Qingwen Ni. Determination of cortical bone porosity and pore size distribution using a low field pulsed NMR approach. Journal of Orthopaedic Research 21(2), 312-319. 2003.

15. Zhang, Faming, Chang, Jiang, Lu, Jianxi, Lin, Kaili, and Ning, Congqin. Bioinspired structure of bioceramics for bone regeneration in load-bearing sites. Acta Biomaterialia 3(6), 896-904. 2007.

16. Louis Solomon, David Warwick and Selvadurai Nayagam (2005) Apley's Concise System of Orthopaedics and Fractures, Hodder Headline Group, UK

17. T. Duckworth (1995) Orthopaedics and Fractures, Blackwell Science Ltd, UK

18. Gary Delforge (2002) Musculoskeletal Trauma: Implications for Sports Injury Management, Human Kinetics, USA

19. Novicoff, Wendy M., Manaswi, Abhijit, Hogan, MaCalus V., Brubaker, Shawn M., Mihalko, William M., and Saleh, Khaled J. Critical Analysis of the Evidence for Current Technologies in Bone-Healing and Repair. J Bone Joint Surg Am 90(Supplement_1), 85-91. 2008.

20. B. D. Porter, J. B. Oldham, S.-L. He, and M. E. Zobitz. Mechanical Properties of a Biodegradable Bone Regeneration Scaffold. Journal of Biomechanical Engineering 122(3), 286-288. 2000. American Society of Mechanical Engineers.

21. Kai-Uwe Lewandrowski, Donald L. Wise, Debra J. Trantolo, Joseph D. Gresser, Michael J. Yazemski, and David E. Altoobelli. Tissue Engineering and Biodegradable Equivalents-Scientific and Clinical Applications. 2002. USA, Marcel Dekker Inc. 2002.

22. Finkemeier, Christopher G. Bone-Grafting and Bone-Graft Substitutes. J Bone Joint Surg Am 84(3), 454-464. 2002.

23. Greenwald, A. Seth, Boden, Scott D., Goldberg, Victor M., Khan, Yusuf, Laurencin, Cato T., and Rosier, Randy N. Bone-Graft Substitutes: Facts, Fictions, and Applications. J Bone Joint Surg Am 83, S98-103. 2001.

24. Oxford University Press (2003) Concise colour medical dictionary, Oxford

University Press, UK

25. Hench, L. L. (ii) The challenge of orthopaedic materials. Current Orthopaedics 14(1), 7-15. 2000.

26. M. J. W. Hubble. Bone transplantation. Current Orthopaedics Volume 15(Issue 3), Pages 199-205. 2001.

27. Guelinckx P J and Sinsel N K. The "Eve" procedure: the transfer of vascularized seventh rib, fascia, cartilage, and serratus muscle to reconstruct difficult defects. Plast Reconstr Surg 97(3), 527-35. 96.

28. Mikos, A.G., McIntire, L.V., Anderson, J.M. and Babensee, J.E. (1998) Host response to tissue engineered devices. Adv Drug Deliv Rev 33, 111-139.

29. Erbe, E. M., Marx, J. G., Clineff, T. D., and Bellincampi, L. D. Potential of an ultraporous betatricalcium phosphate synthetic cancellous bone void filler and bone marrow aspirate composite graft. Eur Spine J 10 Suppl 2, S141-6. 2001.

30. Giannoudis, Peter V., Dinopoulos, Haralambos, and Tsiridis, Eleftherios. Bone substitutes: An update: Proceedings from the 1st European Clinical Symposium on Bone and Tissue Regeneration 27-28 November 2004. Injury 36(3, Supplement 1), S20-S27. 2005.

31. Botez, P., Sirbu, P., Simion, L., Munteanu, Fl., and Antoniac, I. Application of a biphasic macroporous synthetic bone substitutes CERAFORM: clinical and histological results. European journal of orthopaedic surgery and traumatology

19(6), 387-395. 2009.

32. Livingston, T., Ducheyne, P., and Garino, J. In vivo evaluation of a bioactive scaffold for bone tissue engineering. J Biomed Mater Res 62(1), 1-13. 2002.

33. Livingston, T., Ducheyne, P., and Garino, J. In vivo evaluation of a bioactive scaffold for bone tissue engineering. J Biomed Mater Res 62(1), 1-13. 2002.

34. Sarazin, Pierre, Roy, Xavier, and Favis, Basil D. Controlled preparation and properties of porous poly(-lactide) obtained from a co-continuous blend of two biodegradable polymers. Biomaterials 25(28), 5965-5978. 2004.

35. Gogolewski, S. Bioresorbable polymers in trauma and bone surgery: Bioresorbierbare Polymere in der Trauma- und Knochenchirurgie: Polymeres bioresorbables en traumatologie et chirurgie orthopedique: Los polimeros biorreabsorbibles en la cirugia osea y traumatologica. Injury 31(Supplement 4), D28-D32. 2000.

36. Buddy D. Ratner, Allan S. Hoffman, Frederick J. Schoen and Jack E. Lemons (2004) Biomaterials Science: An Introduction to Materials in Medicine, Elsevier Inc.,

37. Todo, Mitsugu, Park, Sang Dae, Arakawa, Kazuo, and Takenoshita, Yasuharu. Relationship between microstructure and fracture behavior of bioabsorbable HA/PLLA composites: The 11th US-Japan Conference on Composite Materials. Composites Part A: Applied Science and Manufacturing 37(12), 2221-2225. 2006.

38. C. Mauli Agrawal and Kyriacos A. Athanasiou. Technique to control pH in vicinity of biodegrading PLA-PGA implants. Journal of Biomedical Materials Research 38(2), 105-114. 97.

39. Pamela Habibovic and Klaas de Groot. Osteoinductive biomaterials-properties and relevance in bone repair. Journal of Tissue Engineering and Regenerative Medicine 1(1), 25-32. 2007.

40. Habibovic, Pamela, Gbureck, Uwe, Doillon, Charles J., Bassett, David C., van Blitterswijk, Clemens A.,and Barralet, Jake E. Osteoconduction and osteoinduction of low-temperature 3D printed bioceramic implants. Biomaterials 29(7), 944-953. 2008.

41. Larry L. Hench and June Wilson (1999) An Introduction to Bioceramics, World Scientific Publishing Co., UK

42. Rezwan, K., Chen, Q. Z., Blaker, J. J., and Boccaccini, Aldo Roberto. Biodegradable and bioactive porous polymer/inorganic composite scaffolds for bone tissue engineering. Biomaterials 27(18), 3413-3431. 2006.

43. Hench, Larry L. Genetic design of bioactive glass. Journal of the European Ceramic Society 29(7), 1257-1265. 2009.

44. Bucholz, Robert W. MD. Nonallograft Osteoconductive Bone Graft Substitutes. Clinical Orthopaedics & Related Research February 395, 44-52. 2002.

45. William R. Moore, Stephen E. Graves, and Gregory I. Bain. Synthetic bone

graft substitutes. ANZ Journal of Surgery 71(6), 354-361. 2001. Blackwell Publishing Ltd.

46. Vacanti, Joseph P and Langer, Robert. Tissue engineering: the design and fabrication of living replacement devices for surgical reconstruction and transplantation. The Lancet 354(Supplement 1), S32-S34. 99.

47. Leong, K. F., Cheah, C. M., and Chua, C. K. Solid freeform fabrication of three-dimensional scaffolds for engineering replacement tissues and organs. Biomaterials 24(13), 2363-2378. 2003.

48. Bonnevialle P, Abid A, Mansat P, Verhaeghe L, Cle´ment D,Mansat M. Oste´otomie tibiale de valgisation par addition mediale d'un coin de phosphate tricalcique. Revue de Chirurgie Orthope´dique 2002;88:486 - 492.

49. Galois L, Mainard D, Cohen P, Delagoutte J-P. 23 cas d'utilisation du phosphate tricalcique pour le comblement des pertes de substance osseuse au pied. Med Chir Pied 2001;17:44 - 53.

50. Galois L, Mainard D, Delagoutte J-P. -Tricalcium phosphate ceramic as a bone substitute in orthopaedic surgery. Int Orthop (SICOT) 2002;26:109 - 115.

51. Le Huec J-C, Langlois V, Liquois F, Lesprit E, Cle´ment D. Arthrode'se intersomatique cervicale par greffon en phosphate tricalcique- etude re´trospective de 33 cas. 1 a' 3 ans de recul. Rachis 2001;13/3:197 - 202.

52. Le Huec JC, Lesprit E, Delavigne C, Cle´ment D, Chauveaux D, Le Rebeller A.

Tricalcium phosphate ceramics and allografts as bone substitutes for postero-lateral spine fusion in idiopathic scoliosis: Comparative clinical results at 4 years. Acta Orthop Belg 1997;63/3:202 - 211.

53. Daniels AU, Andriano KP, Smutz WP, Chang MK, Heller J. Evaluation of absorbable poly(ortho esters) for use in surgical implants. J Appl Biomater 1994;5:51 - 64.

54. Bergsma JE, de Bruijn WC, Rozema FR, Bos RR, Boering G. Late degradation tissue response to poly(l-lactide) bone plates and screws. Biomaterials 1995;16:25 - 31.

55. Bos RR, Rozema FR, Boering G, Nijenhuis AJ, Pennings AJ, Verwey AB, Nieuwenhuis P, Jansen HW. Degradation of and tissue reaction to biodegradable poly(l-lactide) for use as internal fixation of fractures: A study in rats. Biomaterials 1991;12:32 - 36.

56. Fuchs M, Koster G, Krause T, Merten HA, Schmid A. Degradation of and intraosseous reactions to biodegradable poly-llactide screws: A study in minipigs. Arch Orthop Trauma Surg 1998;118:140 - 144.

57. Paivarinta U, Bostman O, Majola A, Toivonen T, Tormala P, Rokkanen P. Intraosseous cellular response to biodegradable fracture fixation screws made of polyglycolide or polylactide. Arch Orthop Trauma Surg 1993;112:71 - 74.

58. Peltoniemi HH, Hallikainen D, Toivonen T, Helevirta P, Waris T. SR-PLLA and SR-PGA miniscrews: Biodegradation and tissue reactions in the calvarium and

duramater. J Craniomaxillofac Surg 1999;27:42 - 50.

59. Schakenraad JM, Hardonk MJ, Feijen J, Molenaar I, Nieuwenhuis P. Enzymatic activity towards poly(l-lactic acid) implants. J Biomed Mater Res 1990;24:529 - 545.

60. Van der Elst M, Klein CPAT, De Blieck-Hogervorst JM, Patka P, Haarman HJTM. Bone tissue response to biodegradable polymers used for intra medullary fracture fixation: A long term in vivo study in the sheep femora. Biomaterials 1999;20:121 - 128.

61. Bergsma EJ, Rozema FR, Bos RR, de Bruijn WC. Foreign body reactions to resorbable poly(l-lactide) bone plates and screws used for the fixation of unstable zygomatic fractures. J Oral Maxillofac Surg 1993;51:666 - 670.

62. Bostman OM. Osteoarthritis of the ankle after foreign-body reaction to absorbable pins and screws: A three- to nine-year follow-up study. J Bone Joint Surg Br 1998;80:333 - 338.

63. Bostman OM, Philajamaki HK. Adverse tissue reactions to bioabsorbable fixation devices. Clin Orthop 2000;371:216 - 227.

64. Lajtai G, Noszian I, Humer K, Unger F, Aitzetmuller G, Orthner E. Serial magnetic resonance imaging evaluation of operative site after fixation of patellar tendon graft with bioabsorbable interference screws in anterior cruciate ligament reconstruction. Arthroscopy 1999;15:709 - 718.

65. Martinek V, Friederich NF. Tibial and pretibial cyst formation after anterior cruciate ligament reconstruction with bioabsorbable interference screw fixation. Arthroscopy 1999;15:317 - 320.

66. Takizawa T, Akizuki S, Horiuchi H, Yasukawa Y. Foreign body gonitis caused by a broken poly-l-lactic acid screw. Arthroscopy 1998;14:329,330.

67. Furukawa T, Matsusue Y, Yasunaga T, Nakagawa Y, Okada Y, Shikinami Y, Okuno M, Nakamura T. Histomorphometric study on high-strength hydroxyapatite/poly(l-lactide) composite rods for internal fixation of bone fractures. J Biomed Mater Res 2000;50:410 - 419.

68. Higashi S, Yamamuro T, Nakamura T, Ikada Y, Hyon SH, Jamshidi K. Polymer-hydroxyapatite composites for biodegradable bone fillers. Biomaterials 1986;7:183 - 187.

69. Ignjatovic N, Savic V, Najman S, Plavgic M, Uskokovic D. A study of HAp/PLLA composite as a substitute for bone powder, using FT-IR spectroscopy. Biomaterials 2001;22:571 - 575.

70. Kikuchi M, Tanaka J, Koyama Y, Takakuda K. Cell culture test of TCP/CPLA composite. J Biomed Mater Res 1999;48:108 - 110.

71. Lin FH, Chen TM, Lin CP, Lee CJ. The merit of sintered PDLLA/TCP composites in management of bone fracture internal fixation. Artif Organs 1999;23:186 - 194.

72. Ma PX, Zhang R, Xiao G, Franceschi R. Engineering new bone tissue in vitro on highly porous poly(-hydroxyacids)/hydroxyapatite composite scaffolds. J Biomed Mater Res 2001;54:284 - 293.

73. Rizzi SC, Heath DJ, Coombes AG, Bock N, Textor M, Downes S. Biodegradable polymer/hydroxyapatite composites: Surface analysis and initial attachment of human osteoblasts. J Biomed Mater Res 2001;55:475 - 486.

74. Verheyen CCPM, Wijn de JR, Blitterswijk van CA, Groot de K, Rozing PM. Evaluation of hydroxyapatite/poly(l-lactide) composites: An animal study on push-out strength and interface histology. J Biomed Mater Res 1993;27:433 - 444.

75. Yasunaga T, Matsusue Y, Furukawa T, Shikinami Y, Okuno M, Nakamura T. Bonding behavior of ultrahigh strength unsintered hydroxyapatite particles/poly(l-lactide) composites to surface of tibial cortex in rabbits. J Biomed Mater Res 1999;47:412 - 419.

76. M. Kucharska, Beata Butruka, Katarzyna Walenkoa, Tomasz Brynkb, Tomasz Ciacha. Fabrication of in-situ foamed chitosan/β-TCP scaffolds for bone tissue engineering application Mater. Lett. 85 (2012) 124 - 127.

77. M. Stoppato, Matteo Stoppato, Eleonora Carletti, Viktoryia Sidarovich, Alessandro Quattrone, Ronald E Unger, Charles J Kirkpatrick, Claudio Migliaresi, Antonella Motta, Influence of scaffold pore size on collagen I development: A new in vitro evaluation perspective. J. Bioact. Compat. Pol. 28 (2013) 16 - 32.

78. H. Cao, N. Kuboyama, A biodegradable porous composite scaffold of PGA/β-TCP for bone tissue engineering. Bone 46 (2010) 386 - 395.

79. N. Sultana, M. Wang, Fabrication of HA/PHBV composite scaffolds through the emulsion freezing/freeze-drying process and characterisation of the scaffolds. J. Mater. Sci.: Mater. Med. 19 (2008) 2555 - 2561.

80. D.W. Hutmacher, Scaffolds in tissue engineering bone and cartilage. Biomaterials 21 (2000) 2529 - 2543.

81. H. Yoshikawa, Noriyuki Tamai, Tsuyoshi Murase, Akira Myoui, Interconnected porous hydroxyapatite ceramics for bone tissue engineering. J. R. Soc. Interface 6 (2009) S341 - S348.

82. Loh, Q. L. & Choong, C. Three-dimensional scaffolds for tissue engineering applications: role of porosity and pore size. Tissue Eng Part B Rev 19, 485 - 502 (2013).

83. Cima MJ, Sachs E, Cima LG, Yoo J, Khanuja S, Borland SW, Wu B, Giordano RA. Computer-Derived Microstructures by 3D Printing: Bio-and Structural Materials. In: Proceedings of the Solid Freeform Fabrication Symposium, DTIC Document, The University of Texas at Austin in Austin, Texas. 1994. pp 181 - 190.

84. Griffith LG, Wu B, Cima MJ, Powers MJ, Chaignaud B, Vacanti JP. In vitro organogenesis of liver tissue. Ann N Y Acad Sci 1997;831:382 - 397.

85. Wu BM, Borland SW, Giordano RA, Cima LG, Sachs EM, Cima MJ. Solid free-form fabrication of drug delivery devices. J Controlled Release 1996;40:77 - 87.

86. Kim, S. H. et al. Near-infrared fluorescence imaging for noninvasive trafficking of scaffold degradation. Sci Rep 3, 1198 (2013).

87. Gao J, Dennis JE, Solchaga LA, Awadallah AS, Goldberg VM, Caplan AI. Tissue-engineered fabrication of an osteochondral composite graft using rat bone marrow-derived mesenchymal stem cells. Tissue Eng 2001;7:363 - 371.

88. Solchaga LA, Yoo JU, Lundberg M, Dennis JE, Huibregtse BA, Goldberg VM, Caplan AI. Hyaluronan-based polymers in the treatment of osteochondral defects. J Orthop Res 2000;18:773 - 780.

89. Solchaga LA, Gao J, Dennis JE, Awadallah A, Lundberg M, Caplan AI, Goldberg VM. Treatment of osteochondral defects with autologous bone marrow in a hyaluronan-based delivery vehicle. Tissue Eng 2002;8:333 - 347.

국 문 요 약

3차원 프린팅 기술을 이용한 다공성 폴리락타이드/β-삼인산칼슘 인공지지체의 제작 및 조직공학적 골형성에 관한 연구

최근 조직공학 분야에서는 다양한 재료들을 이용하여 인공지지체를 제작하는 연구가 활발히 이루어지고 있다. 조직공학은 손상된 조직이나 기관의 복원을 도울 수 있는 생체물질, 생물학적, 그리고 공학적인 기술을 다루는 학문을 기반으로 한 의료분야의 중요한 기술로 알려져 왔다. 그래서 생체의 손상된 기능을 복원, 유지, 그리고 향상하는 것을 목적으로 한 다양한 방법이 연구되고 있다. 조직 공학을 이용하여 조직 재생에 필요한 인공지지체는 세포, 성장인자와 함께 중요한 3대 요소 중 하나로 정의된다. 이러한 조직의 회복 및 재생을 위해 제작된 인공지지체는 세포의 원활한 증착과 증식이 이루어지도록 유도하는 것이 필수적이다. 인공지지체 제작에 필요한 재료들은 생분해성 (Biodegradability)과 생체적합성 (Biocompatibility)의 성질을 가지고 있어야 하며, 골과 유사한 기계적 특성도 지니고 있어야 한다. 그리고 조직의 회복 및 재생을 위해 제작된 인공지지체는 우수한 공극을 가지는 내 외부 구조에 주입 된 세포가 부착 및 분화, 그리고 증식에 적합한 환경을 제공해야 한다. 많은 연구자들이 현재 다양한 생체적합성 재료를 이용하여 조직의 특성에 맞는 인공지지체 제작을 위한 연구를 수행하고 있다. 인공지지체 제작을 위해 주로 사용되는 고분자 재료로는 천연고분자와 합성고분자 재료로 분류된다. 천연 물질, 동물, 그리고 인체에서 유래한 천연고분자 재료는 타 재료에 비해 우수한 생체적합성을 지니고 있으며 독성이 없다는 장점을 가지고 있다. 그 종류에는 젤라틴 (Gelatin), 콜라겐 (Collagen), 피브린 (Fibrin), 엘라

스틴 (Elastin), 그리고 알긴산 (Alginate) 등이 있다. 천연고분자에 비해 합성고분자 재료는 비교적 값이 싸고 기계적 특성이 우수하며, 생체 내에서 가수 분해되거나 효소에 의해 분해되어 이상적인 지지체용 고분자로의 장점을 가지고 있다. 대표적인 합성고분자 재료에는 Poly(ε-caprolactone) (PCL), Poly(lactide-co-glycolide)(PLGA), Poly(lactic acid)(PLA) 등이 있다. 특히, 골 조직 재생을 위해 사용되는 고분자 재료인 폴리락타이드와 바이오 세라믹 재료인 트리칼슘 포스페이트(Tricalcium phosphate, TCP)를 이용하여 골 조직 재생을 위한 다양한 인공지지체를 제작하고 있다. 골 조직 재생을 위한 바이오 세라믹 재료인 β-TCP는 뼈와 치아의 무기질과 같은 비슷한 조성을 갖고 있어 구조적으로 안정성을 띄고 있다. 또한, 인체 내에서 신생 골 성장과 동시에 완전히 흡수되는 장점을 가지면서 그 어떤 재료보다 생체 친화성과 활성이 뛰어나다고 알려져 왔다. 하지만 고체로 이루어져 있어 열을 이용하여 제작할 수 있는 고분자 재료에 비해 바이오 세라믹 재료는 파우더로 이루어져 있어 고분자로 만들어진 인공지지체보다 기계적 강도가 떨어지는 단점을 가지고 있다. 또한, 재료가 파우더로 구성되어 있어 내부 공극이 우수한 3차원 인공지지체를 제작하는 데에 많은 어려움이 있다. 그래서 이를 보완하고자 세라믹 재료를 고분자 재료와 혼합하여 제작하는 연구가 많이 이루어지고 있다. 본 연구에서는 고분자 재료인 PLA와 바이오 세라믹 재료인 β-TCP를 혼합한 3차원 인공지지체를 3차원 프린팅 시스템을 이용하여 제작하였다. 3차원 프린팅 시스템은 마이크로 단위의 원하는 3차원 형상 구조물을 제작하기 위한 시스템으로서 정밀하고 신속한 제어를 가능하게 한다. 또한 공압, 온도, 그리고 이동속도에 따라 적층되는 재료의 선폭과 선 높이를 결정지을 수 있는 장점을 가지고 있다. 일반적으로 폴리머와 생체세라믹을 혼합하여 3차원 프린팅 시스템으로 지지체를 제조할 경우 세라믹 재료의 함유량은 한계가 있다. 이는 생체 세라믹 파우더가 증가하면 노즐을 통한 토출의 어려움이 있기 때문에 생체 세라믹 파우더의 양 조절과 혼합방법은 매우 중요한 부분이다. 본 연구에서는 3차원 프린팅 시스템을 이용하여 PLA 고분자 재료에 β-TCP 바이오 세라믹 재료가 70%까지 혼합된 3차원 인

공지지체를 제작하고 지지체의 특성과 골형성능을 평가하였다. 제작된 인공지지체는 전자주사현미경으로 원하는 크기의 기공에 맞게 잘 제작된 것을 확인할 수 있었으며, 압축강도 분석을 통해 해면골의 압축강도와 유사함을 확인하였다. 제작된 PLA/β-TCP 지지체의 세포적합성을 평가하기 위해 세포증식 및 부착능 실험을 진행하였고, β-TCP의 함량이 증가할수록 세포적합성은 가장 높게 나타났다. 이러한 결과는 골 전도성이 우수한 β-TCP의 재료 특성 상 세포 증식률이 좋은 것으로 여겨진다. β-TCP가 70% 혼합된 PLA/β-TCP 인공지지체의 골 재생능을 평가하기 위해 랫드 두개골 결손모델과 토끼 대퇴골 결손모델에 인공지지체를 이식 후 Micro-CT와 조직염색 분석을 실시한 결과, 골 조직의 정량 분석에서 β-TCP 함량이 증가할수록 신생골의 부피가 증가하는 것을 확인 할 수 있었다. 이상의 결과 3차원 프린팅 시스템을 이용하여 제조된 PLA/TCP 지지체는 골재생 및 치유에 효과적임을 확인할 수 있었다.

핵심되는 말 : 폴리락티산, 삼인삼칼슘, 3차원 적층 시스템, 조직공학, 인공지지체